Toxicology Letters 228 (2014) 235–240

Contents lists available at ScienceDirect

Toxicology Letters

journal homepage: www.elsevier.com/locate/toxlet

Peroxisome proliferator-activated receptor α mediates di-(2-ethylhexyl) phthalate transgenerational repression of ovarian *Esr1* expression in female mice

Michihiro Kawano[a,b,1], Xian-Yang Qin[a,1], Midori Yoshida[c], Tomokazu Fukuda[d], Hiroko Nansai[a], Yumi Hayashi[e], Tamie Nakajima[f], Hideko Sone[a,*]

[a] Research Center for Environmental Risk, National Institute for Environmental Studies, Tsukuba, Ibaraki, Japan
[b] Department of Nursing, School of Health Sciences, Ibaraki Prefectural University of Health Science, Inashiki-gun, Ibaraki, Japan
[c] Division of Pathology, Biological Safety Research Center, National Institute of Health Sciences, Setagaya-ku, Tokyo, Japan
[d] Department of Animal Production Science, Graduate School of Agricultural Science, Tohoku University, Sendai, Miyagi, Japan
[e] Pathophysiological Laboratory Sciences, Department of Radiological and Medical Laboratory Sciences, Nagoya University Graduate School of Medicine, Nagoya, Aichi, Japan
[f] College of Life and Health Sciences, Chubu University, Kasugai, Aichi, Japan

HIGHLIGHTS

- Effect of DEHP on ovarian gene expression is measured in PPARα knockout mice.
- Transgenerational repression of ovarian Esr1 expression by DEHP is found in WT mice.
- DEHP regulation of ovarian Esr1 gene expression is lost in PPARα-knockout mice.
- Transgenerational effect of DEHP is partly mediated by PPARα-dependent pathways.

ARTICLE INFO

Article history:
Received 19 October 2013
Received in revised form 20 April 2014
Accepted 23 April 2014
Available online 5 May 2014

Keywords:
DEHP
PPARα
Transgenerational
Female mice
Reproductive

ABSTRACT

Di-(2-ethylhexyl)-phthalate (DEHP) is a phthalate ester that binds peroxisome proliferator-activated receptor α (PPARα) to induce proliferation of peroxisomes and regulate the expression of specific target genes. The question of whether the effect of DEHP on female reproductive processes is mediated via PPARα-dependent signaling is controversial. In this study, we investigated the effect of exposure to DEHP on ovarian expression of estrogen receptor α (*Esr1*) and aromatase (*Cyp19a1*) in three generations of Sv/129 wild-type (WT, +/+) and PPARα (−/−) knockout mice. Compared with untreated controls, ovarian expression of *Esr1* decreased in response to DEHP treatment in the F0 (0.56-fold, $P=0.19$), F1 (0.45-fold, $P=0.023$), and F2 (0.35-fold, $P=0.014$) generations of WT mice, but not PPARα-null mice. Our data indicate that transgenerational repression by DEHP of ovarian *Esr1* gene expression is mediated by PPARα-dependent pathways. Further studies are required to elucidate the mechanisms underlying crosstalk between PPARα and Esr1 signaling in reproductive processes.

© 2014 Elsevier Ireland Ltd. All rights reserved.

1. Introduction

Because of their common industrial application as plasticizers, phthalates esters are highly prevalent in the environment (Halden, 2010). Di-(2-ethylhexyl)-phthalate (DEHP), which is commonly used as a plasticizer of polyvinyl chloride (PVC), has been characterized as an endocrine disruptor on the basis of its anti-androgen activity (Fisher, 2004). Given its ability to cross the placenta and pass into breast milk, considerable concern has been raised over the potential harm to the developing fetus and newborn arising from exposure to DEHP (Adibi et al., 2008). Several well-designed epidemiological studies have consistently documented the anti-androgenic effects of prenatal exposure to DEHP on indices of male reproductive development, such as decreased anogenital index (AGI) in male neonates (Suzuki et al., 2012; Swan, 2008; Swan et al., 2005). Occupational exposure to DEHP also showed positive associations with sperm DNA denaturation induction and negative

* Corresponding author. Tel.: +81 29 850 2464; fax: +81 29 850 2546.
E-mail address: hsone@nies.go.jp (H. Sone).
[1] These authors contributed equally.

http://dx.doi.org/10.1016/j.toxlet.2014.04.019
0378-4274/© 2014 Elsevier Ireland Ltd. All rights reserved.

associations with sperm motility (Huang et al., 2011). However, no significant relationships between prenatal exposure to DEHP and birth outcomes were also reported (Suzuki et al., 2010). Although there has been a controversy about its toxicity, many scientific and professional organizations have made recommendations to reduce DEHP exposure in pregnant women and young children to prevent unexpected consequences of reproductive and development effects in the offspring (Braun et al., 2013).

In rodents, it has become apparent that DEHP exposure might affect the development of reproductive tract by decreasing fetal testosterone synthesis during sexual differentiation in male rats and mice (Wolf et al., 1999; Wu et al., 2012; Zacharewski et al., 1998). Exposure to DEHP *in utero* and during lactation at dose levels relevant to humans also causes a significant delay in indices of pubertal onset in female offspring rats, such as vaginal opening (Miller and Auchus, 2011). Moreover, long-term DEHP exposure has been associated with reduced serum levels of estradiol, follicle-stimulating hormone (FSH), pituitary FSH and luteinizing hormone in female rats (Andrade et al., 2006). Despite these studies, comprehensive information on the molecular mechanism underlying the potential endocrine disruptive effect of low-dose DEHP exposure on reproductive function in female animal model is lacking.

Peroxisome proliferator-activated receptor α (PPARα), a ligand-regulated member of the nuclear receptor superfamily of transcription factors, was the first of three members of the PPAR family identified in the 1990s (Arcadi et al., 1998). By modulating the expression of peroxisomal lipid metabolism and growth regulatory genes, activation of PPARs plays an important role in the metabolism of xenobiotics (Lovekamp-Swan and Davis, 2003). Consistent with weak PPARα agonism of DEHP (Haynes-Johnson et al., 1999), we have previously shown that hepatic PPARα is required for the toxic effect of maternal exposure to DEHP in male offspring mice (Hayashi et al., 2011). Moreover, PPARα transcript is also related to the effect of DEHP on metabolism and fertility in female mice (Schmidt et al., 2012). On the other hand, recent evidences also indicated that DEHP can induce liver tumorigenesis through a PPARα-independent pathway (Ito et al., 2007). These studies aside however, the role of PPARα in the developmental and reproductive toxicity associated with DEHP exposure is unclear (Kobayashi et al., 2009). Accordingly, to clarify the potential role of PPARα in the effects of DEHP on female reproductive health, we compared the transgenerational effect of DEHP on ovarian gene expression in wild-type (WT, +/+) and PPARα (−/−) knockout mice.

2. Materials and methods

2.1. Experimental animals

Experiments in this study were conducted according to the Guidelines for Animal Experiments of Shinshu University, Japan. WT and PPARα knockout mice in the Sv/129 genetic background were generated as described elsewhere (Lee et al., 1995). Animal husbandry was performed in a clean room with controlled temperature, relative humidity, and light with 12-h light/dark cycle, as previously described (Hayashi et al., 2011).

2.2. DEHP exposure

DEHP (CAS No. 117-82-7) was purchased from Wako Pure Chemistries (Osaka, Japan). Corn oil (Sigma Chemical Company, St. Louis, MO, USA) was used as the vehicle control. Mating was set up according to the schedule previously described (Hayashi et al., 2011). WT and PPARα knockout mice were given a diet containing vehicle control or 0.05% DEHP (approximately 80 mg/kg/day) through three generations ($n = 6$ in each group in each generation). DEHP was administered starting in the F0 generation at 12 weeks of age and continuing to the end of experiment in the F2 generation. Mice were sacrificed by CO_2 asphyxiation at 36 weeks of age in the F0 generation and at 16 weeks of age in the F1 and F2 generations (Fig. 1). Blood samples were taken from the abdominal aorta and plasma was separated by centrifugation at 4 °C and stored at 80 °C until assay for testosterone and estradiol. Body and organs such as liver and ovaries were dissected out and weighed as quickly as possible. Then ovarian tissue samples for RNA analysis were separated into two sections, one of which was snap-frozen in liquid nitrogen and stored at −80 °C, while the other was fixed in buffered formalin for 6–24 h. Concentrations of testosterone and estradiol in plasma were measured by a testosterone or estradiol EIA kit (Cayman, Ann Arbor, MI).

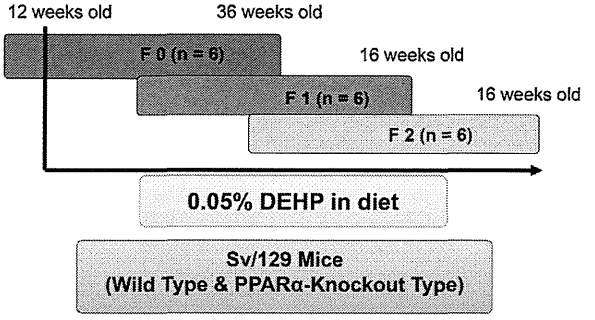

Fig. 1. Schedule of transgenerational exposure to dietary DEHP. Maternal mice of both genotypes in the F0 generation were exposed to DEHP in their diet from 16 to 36 weeks of age. Offspring (F1) and third-generation (F2) mice were also exposed to dietary DEHP until 16 weeks of age.

2.3. Quantitative real-time reverse transcription-polymerase chain reaction (RT-PCR)

Total RNA was isolated from a frozen ovary using an ISOGEN kit from NIPPON GENE (Tokyo, Japan) following instructions from the manufacturer. Quantification and quality assessment of the isolated RNA samples were performed and verified using an Agilent Bioanalyzer 2100 and an RNA 6000 Nano Assay (Agilent Technologies, Palo Alto, CA, USA) in accordance with the manufacturer's instructions. cDNA was synthesized using random primers (Perkin-Elmer Applied Biosystems Inc., Tokyo, Japan). Oligonucleotide primers and TaqMan probe were designed using Primer Express, version 1.0 (Applied Biosystems, Foster City, CA, USA) and Oligo 5.1 software (National Bioscience, Plymouth, MN, USA) based on GenBank database sequences as follows: *Esr1* (Accession # M38651), primer sequences 5′-tcaactgggcaaagagagtg-3′ and 5′-gtgctggacagaaacgtgta-3′ TaqMan probe sequences 5′-agtgtgcctggctggagattctgatgatt-3′; *Cyp19a1* (aromatase) (Accession # D00659), primer sequences 5′-gaaagagaacgtgaatcagtg-3′ and 5′-atgatgttagttccctttta-3′, TaqMan probe sequences 5′-ttaatgaaagcatgcggtaccagcct-3′; *Gapdh* (Accession# M32599), primer sequences 5′-tgcagtggcaaagtggagatt-3′ and 5′-gttgaatttgccgtgagtggag-3′ TaqMan probe sequences 5′-ccatcaacgacccctt-3′. The amplification reaction was performed in an ABI PRISM 7000 Sequence Detector (Applied Biosystems) under the following cycling conditions: 95 °C for 10 min, followed by 50 cycles of 95 °C for 15 s, 56 °C for 1 min and 72 °C for 30 s. The gene expression levels were calculated based on the threshold cycle using Sequence Detection System Software (Applied Biosystems). Gene expression was normalized according to *Gapdh* expression levels.

2.4. Histological analysis

Ovarian tissue samples fixed in 10% neutral buffered formalin were embedded in paraffin and sliced into 5-μm sections. Three sections on the cut surface of the maximum width diameter of ovary per animal were observed. The number of follicles in one slice out of three was counted. Ovarian tissue sections were stained with hematoxylin and eosin and the number and size of follicle and corpus luteum were examined under a light microscope using an Olympus BX50 (Olympus, Tokyo, Japan).

2.5. Bioinformatics and statistical analysis

Quantitative data were expressed as the mean ± standard deviation. For body and organs weight, hormone concentrations, multiple comparisons were made between the exposure groups and the control group using Dunnett's test after one-way ANOVA. Statistical analysis was performed by the two-tailed Student's *t*-test. Relationships were considered statistically significant at $P < 0.05$. Molecular network underlying the reproductive effect of DEHP was analyzed using the Ingenuity Pathway Analysis program (Ingenuity Systems, Mountain View, CA, USA).

3. Results

3.1. Transgenerational effect of DEHP exposure on body, liver, ovary weights, and sex hormones in WT and PPARα knockout mice

No abnormalities were apparent during clinical observation in any generation of WT and PPARα knockout DEHP-treated mice

Table 1
Generational comparison of body, liver, ovary weights, and sex hormones in female WT and PPARα knockout mice[a].

Generation	F0 control	F0 DEHP	F1 control	F1 DEHP
WT				
Number of mice	6	6	6	6
Body weight	28.0 ± 3.7	30.2 ± 1.3	26.7 ± 1.3	22.7 ± 2.2
Liver weight	0.87 ± 0.07	1.04 ± 0.11	0.93 ± 0.04	0.73 ± 0.09
Liver/body (%)	3.12 ± 0.14	3.46 ± 0.24	3.49 ± 0.01	3.19 ± 0.14
Ovary weight	0.014 ± 0.0001	0.014 ± 0.0000	0.015 ± 0.0020	0.014 ± 0.0010
Ovary/body (%)	0.048 ± 0.007	0.047 ± 0.003	0.054 ± 0.004	0.061 ± 0.006
Testosterone (ng/mL)	0.20 ± 0.08	0.45 ± 0.07	0.10 ± 0.05	0.22 ± 0.06
Estradiol (pg/mL)	27 ± 5	49 ± 18	22 ± 5	38 ± 11
PPARα-knockout				
Number of mice	6	6	6	6
Body weight	26.0 ± 1.6	31.8 ± 2.6	21.0 ± 0.9	23.4 ± 3.7
Liver weight	0.94 ± 0.21	1.51 ± 0.17	0.71 ± 0.05	0.71 ± 0.10
Liver/body (%)	3.60 ± 0.58	4.75 ± 0.52	3.40 ± 0.34	3.05 ± 0.17
Ovary weight	0.015 ± 0.004	0.017 ± 0.003	0.013 ± 0.004	0.015 ± 0.0020
Ovary/body (%)	0.059 ± 0.010	0.055 ± 0.008	0.061 ± 0.018	0.063 ± 0.010
Testosterone (ng/mL)	0.15 ± 0.07	0.23 ± 0.06	0.10 ± 0.04	0.20 ± 0.14
Estradiol (pg/mL)	26 ± 11	26 ± 4	21 ± 6	28 ± 4

[a] Mean ± standard deviation. Significant differences from control for all data except the sex hormones were performed by the Dunnett's test.
[b] Number of animals for testosterone and estradiol data were two to four in each group.

prior to sacrifice and necropsy. Similarly, DEHP treatment had no significant effect on body, liver, and ovary weight in female dams (F0) and offspring (F1) in either WT or PPARα knockout mice. Of interest, increase of circulating estradiol was observed only in WT but not PPARα knockout mice (Table 1).

3.2. Effect of DEHP on ovarian Esr1 expression in WT and PPARα knockout mice

We next examined the effect of DEHP exposure on ovarian *Esr1* gene expression in WT and PPARα knockout mice (Fig. 2). Compared with controls, ovarian *Esr1* expression decreased in response to dietary 0.05% DEHP in the F0 (0.56-fold, $P = 0.19$), F1 (0.45-fold, $P = 0.023$), and F2 (0.35-fold, $P = 0.014$) generations of WT mice. In contrast, DEHP had no significant on ovarian *Esr1* gene expression in either the F0 (1.49-fold, $P = 0.18$), F1 (1.00-fold, $P = 0.49$), or F2 (0.80-fold, $P = 0.27$) generations of PPARα knockout mice.

3.3. Effect of DEHP on the ovarian Cyp19a1 (aromatase) gene expression in F2 mice

Next, we compared the effect of DEHP exposure on ovarian *Cyp19a1* (aromatase) gene expression in WT and PPARα knockout F0 dams (Fig. S1) and the F2 generation (Fig. 3). We observed no statistically significant changes of ovarian *Cyp19a1* expression in response to DEHP treatment in both WT and PPARα knockout mice.

Supplementary figure related to this article can be found, in the online version, at http://dx.doi.org/10.1016/j.toxlet.2014.04.019.

3.4. Histopathological examination of ovaries of F2 mice exposed to DEHP

Histopathological analysis of uteri and ovaries from F0, F1, and F2 WT and PPARα knockout mice treated with control diet or 0.05%

Table 2
Histopathological findings in F0, F1, and F2 female WT and PPARα knockout mice.

Generation & PPARα genotype treatment group	No of mice	Ovary							Uterus						
		Corpus luteum			Follicles				Similar histology to cycle						
		Total	New	Old	Graafian	Medium	Small	Atresia	P	E	M	M/D	D	D/P	Others
F0 WT															
Control	3	2.3 ± 2.1	2.3 ± 2.1	0	−/+	−/+	+/++	+/++	1		2				
DEHP	4	2.8 ± 2.4	1.8 ± 2.0	1 ± 0.7	−/+	−/++	+/++	+/++	2				2		
F0 PPARα-knockout															
Control	3	2.3 ± 0.9	2 ± 0.8	0.3 ± 0.5	−/+	−/++	+/++	+/++			1	1		1	
DEHP	4	4.0 ± 3.1	NE1	NE1	−/+	−/++	+/++	−/+/++		1	2			1	
F1 WT															
Control	3	3.7 ± 1.2	3.7 ± 1.2	0	−/+	+	+/++	+/++	1		1		1		
DEHP	7	2.9 ± 1.5	2.6 ± 1.2	0.3 ± 0.7	−/+	−/+	+/++	++	1	2	3		1		
F1 PPARα-knockout															
Control	3	10 ± 0.8	0.3 ± 0.5	0.7 ± 0.9	−/+	+	++	+/++	1		1	1			
DEHP	5	1.4 ± 0.8	1.4 ± 0.8	0	−/+	−/+	+/++	+/++	2	1		1		1	
F2 WT															
Control	5	43 ± 0.8	NE1	NE1	−	+/++	+	+	NE2						
DEHP	5	1.8 ± 0.4	NE1	NE1	−	+/++	+/++	+/++	NE2						
F2 PPARα-knockout									NE2						
Control	5	3.2 ± 0.8	NE1	NE1	−	+	+	+/++	NE2						
DEHP	5	2.0 ± 1.1	NE1	NE1	−	+/++	+	+/++	NE2						

NE1: not available for detailed classification; NE2, not examined. Similar morphology in the uterus to those at P, proestrus; E, estrus; M, metestrus; D, diestrus.

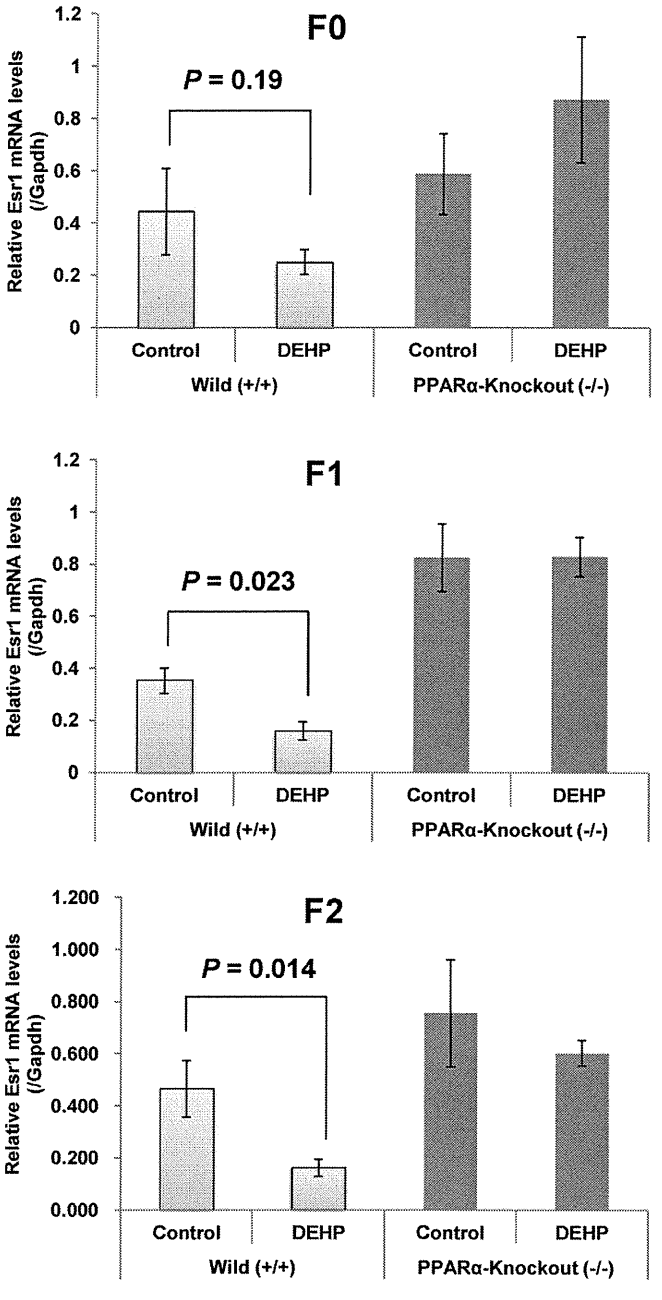

Fig. 2. Effect of DEHP on ovarian *Esr1* gene expression in WT and PPARα knockout mice. Gene expression levels were normalized to GAPDH and values are reported as mean ± standard deviation.

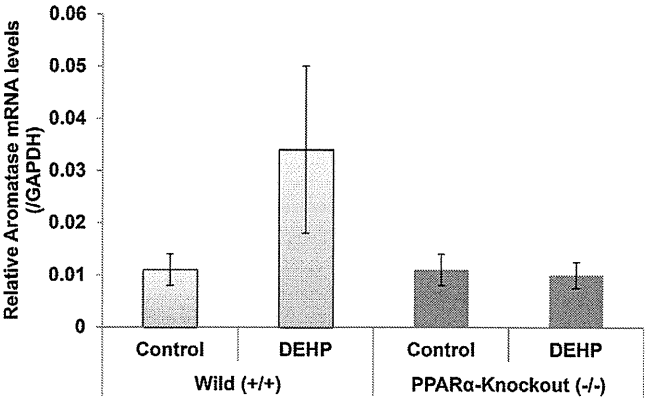

Fig. 3. Effect of DEHP on ovarian aromatase gene expression in WT and PPARα knockout mice. Gene expression levels were normalized to GAPDH and values are reported as mean ± standard deviation.

DEHP diet is shown in Fig. 4 and quantitative data are summarized in Table 2. Although ovary size varied, with those in the F1 generation of control diet-PPARα knockout mice being notably small, most ovaries had corpora lutea and growing follicles, indicating that ovulation and estrous cycle were unaffected by DEHP treatment. Moreover, no morphological differences were observed among genotypes and DEHP treatment. Histopathological examination indicated that DEHP exposure had no significant effect on the number of primary ovarian follicles in either WT or PPARα knockout mice.

4. Discussion

Plastics have become indispensable in modern society, with annual global production exceeding 300 million tons (Halden, 2010). DEHP is the most commonly used phthalate plasticizer for PVC and has been described as an endocrine disruptor for its anti-androgen activity (Fisher, 2004). The public health threat posed by phthalate-tainted foodstuffs is exemplified in Taiwan, where elevated concentrations (~2108 ppm) of DEHP have been detected in a wide variety of food products, including sports drinks, fruit beverages, tea drinks, fruit jam/nectar/jelly, and health food supplements (Wu et al., 2012). To determine the effect of DEHP on female reproductive health, and to clarify the molecular basis of this effect, we set out here to study the transgenerational effect of DEHP on ovarian gene expression in Sv/129 WT and PPARα knockout mice. We found that ovarian *Esr1* expression was reduced in response to DEHP treatment in the F0, F1, and F2 generations of WT mice but not in PPARα-knockout mice, indicating that the adverse transgenerational effects of DEHP on female reproductive health are mediated at least in part by PPARα.

It has been hypothesized that DEHP is an estrogenic endocrine disruptor *in vivo* but not *in vitro* (Wolf et al., 1999; Zacharewski et al., 1998). Consistent with such a notion, we previously found no estrogenic effect of DEHP in Esr1-positive BG1Luc4E2 human

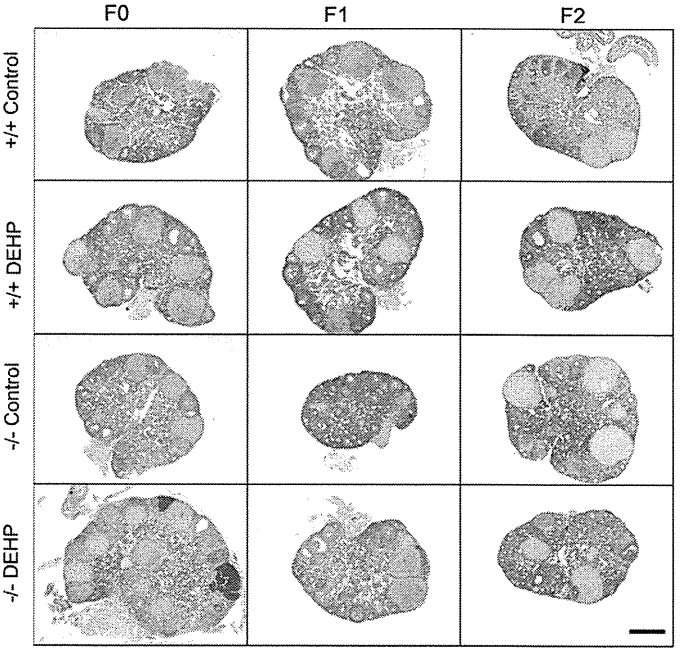

Fig. 4. Ovaries of three generations of WT and PPARα knockout mice in the control and DEHP-treated groups. Scale bar: 50 μm.

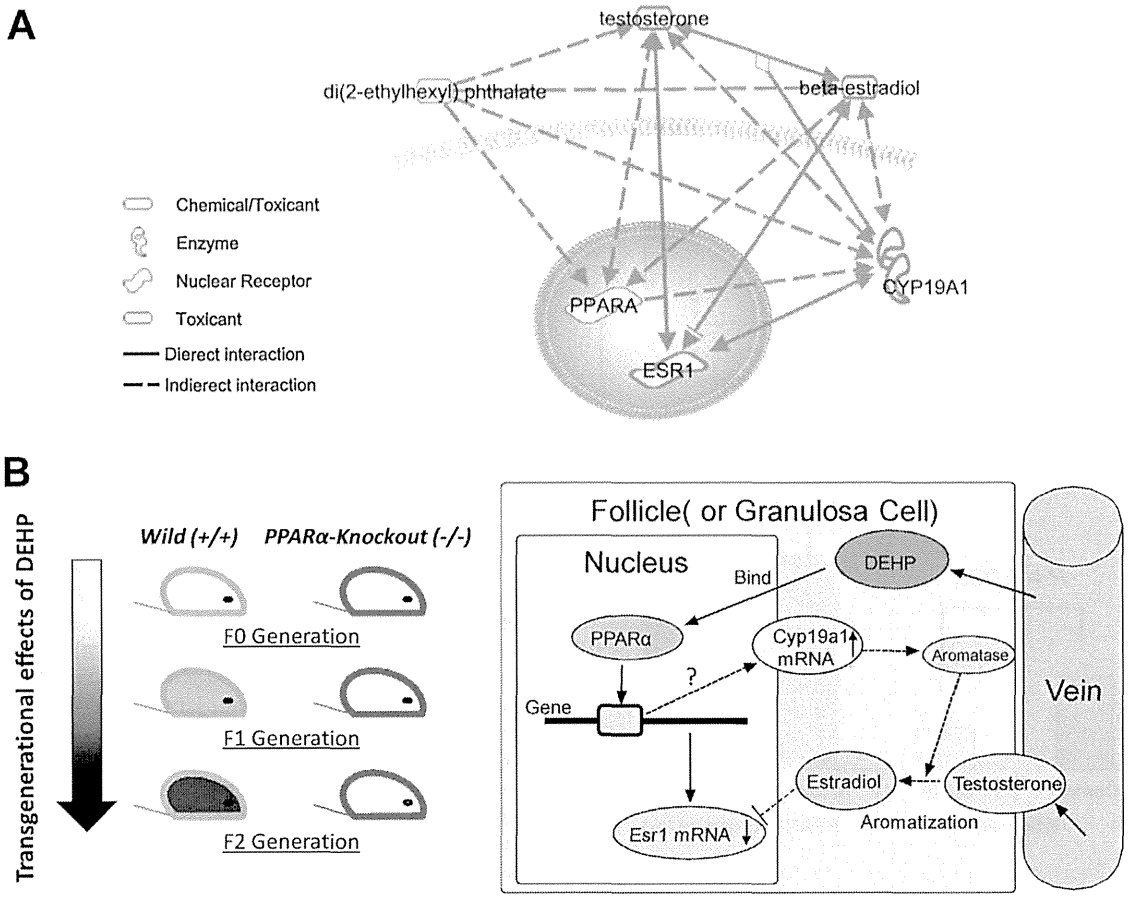

Fig. 5. Schematic diagram of molecular mechanism involved in the reproductive effect of DEHP. (A) The knowledge-based network generated by IPA. (B) Schematic model showing the potential PPARα-dependent pathways of the transgenerational adverse reproductive effects of DEHP in female mice.

ovarian cancer cells at concentrations as high as 0.1 mM (Qin et al., 2011). In contrast, in this present *in vivo* study, increased serum estradiol contents and reduced ovarian *Esr1* gene expression were observed in WT mice fed with 0.05% DEHP (Table 1 and Fig. 2). Aromatase (Cyp19a1) catalyzes the conversion of androstenedione to estrone and testosterone to estradiol (Miller and Auchus, 2011), which are key steps in estrogen biosynthesis. Non-monotonic dose–response effects of DEHP exposure on aromatase activity have been reported in male rats, such that low doses are inhibitory and high doses are stimulatory (Andrade et al., 2006), and it has been suggested that the endocrine-disrupting effect of DEHP development of the male reproductive tract is related to inhibition of testosterone (Arcadi et al., 1998). Production of estradiol, which plays an essential role in female reproductive physiology, is mediated by FSH signaling, which stimulates aromatase activity in ovarian granulosa cells to induce the synthesis of estradiol from testosterone (Haynes-Johnson et al., 1999). Excess estradiol in the ovary has been suggested to inhibit ovarian *Esr1* expression because of the negative feedback regulation of the interaction between Esr1 and its ligand (Kobayashi et al., 2009). According to the IPA knowledgebase, which is an extensive database of functional interactions that are drawn from peer-reviewed publications (Calvano et al., 2005), it is assumed that DEHP activates PPARα to increase ovarian aromatase expression, which in turn promotes the synthesis of estradiol from testosterone. Elevated levels of estradiol subsequently inhibit *Esr1* expression via negative feedback of the Esr1-ligand interaction (Fig. 5). However, as the induction of ovarian aromatase by DEHP observed in our study failed to reach statistical significance, further study is needed to understand the role of aromatase in DEHP-induced adverse reproductive effect.

The PPARα dependence of the effect of DEHP on female reproductive health is a subject of controversy (Kobayashi et al., 2009). For example, while we previously showed that hepatic PPARα is required for the toxic effect of maternal exposure to DEHP in male offspring of mice (Hayashi et al., 2011), DEHP has also been shown to induce liver tumorigenesis via a PPARα-independent pathway (Ito et al., 2007). In the present study, we found that DEHP regulation of ovarian *Esr1* gene expression in WT mice was lost in PPARα-knockout mice, indicating that the transgenerational regulation of ovarian gene expression by DEHP is at least partly PPARα dependent. Consistent with this observation, a recent study showed that reductions in the number of methylated CpG sites of imprinted genes in the oocytes of F1-treated mice oocytes are transferable to F2 offspring, suggesting that DEHP has an epigenetic effect in oocytes (Li et al., 2014).

In summary, our data indicate that transgenerational repression by DEHP of ovarian *Esr1* gene expression is mediated by PPARα-dependent pathways. The possible mechanism might relate with negative feedback of the Esr1-ligand interaction (Fig. 5). Further studies are required to elucidate the crosstalk between PPARα and Esr1 signaling in reproductive processes.

Conflict of interest

The authors declare that there are no conflicts of interest.

Transparency document

The Transparency document associated with this article can be found in the online version.

Acknowledgments

This study was partly supported by the Environmental Rechnology Development Fund (ERTDF R01 H19-21) to H.S. that was granted by the Ministry of Environment, Japan. The funding agency had no role in the study design, data collection and analysis, decision to publish, or preparation of the manuscript.

References

Adibi, J.J., Whyatt, R.M., Williams, P.L., Calafat, A.M., Camann, D., Herrick, R., Nelson, H., Bhat, H.K., Perera, F.P., Silva, M.J., Hauser, R., 2008. Characterization of phthalate exposure among pregnant women assessed by repeat air and urine samples. Environ. Health Perspect. 116, 467–473.

Andrade, A.J., Grande, S.W., Talsness, C.E., Grote, K., Chahoud, I., 2006. A dose–response study following in utero and lactational exposure to di-(2-ethylhexyl)-phthalate (DEHP): non-monotonic dose–response and low dose effects on rat brain aromatase activity. Toxicology 227, 185–192.

Arcadi, F.A., Costa, C., Imperatore, C., Marchese, A., Rapisarda, A., Salemi, M., Trimarchi, G.R., Costa, G., 1998. Oral toxicity of bis(2-ethylhexyl) phthalate during pregnancy and suckling in the Long-Evans rat. Food Chem. Toxicol. 36, 963–970.

Braun, J.M., Sathyanarayana, S., Hauser, R., 2013. Phthalate exposure and children's health. Curr. Opin. Pediatr. 25, 247–254.

Calvano, S.E., Xiao, W., Richards, D.R., Felciano, R.M., Baker, H.V., Cho, R.J., Chen, R.O., Brownstein, B.H., Cobb, J.P., Tschoeke, S.K., Miller-Graziano, C., Moldawer, L.L., Mindrinos, M.N., Davis, R.W., Tompkins, R.G., Lowry, S.F., Inflamm, Host Response to Injury Large Scale Collab. Res, P., 2005. A network-based analysis of systemic inflammation in humans. Nature 437, 1032–1037.

Fisher, J.S., 2004. Environmental anti-androgens and male reproductive health: focus on phthalates and testicular dysgenesis syndrome. Reproduction 127, 305–315.

Halden, R.U., 2010. Plastics and health risks. Annu. Rev. Public Health 31, 179–194.

Hayashi, Y., Ito, Y., Yamagishi, N., Yanagiba, Y., Tamada, H., Wang, D., Ramdhan, D.H., Naito, H., Harada, Y., Kamijima, M., Gonzales, F.J., Nakajima, T., 2011. Hepatic peroxisome proliferator-activated receptor alpha may have an important role in the toxic effects of di(2-ethylhexyl)phthalate on offspring of mice. Toxicology 289, 1–10.

Haynes-Johnson, D., Lai, M.T., Campen, C., Palmer, S., 1999. Diverse effects of tyrosine kinase inhibitors on follicle-stimulating hormone-stimulated estradiol and progesterone production from rat granulosa cells in serum-containing medium and serum-free medium containing epidermal growth factor. Biol. Reprod. 61, 147–153.

Huang, L.P., Lee, C.C., Hsu, P.C., Shih, T.S., 2011. The association between semen quality in workers and the concentration of di(2-ethylhexyl) phthalate in polyvinyl chloride pellet plant air. Fertil. Steril. 96, 90–94.

Ito, Y., Yamanoshita, O., Asaeda, N., Tagawa, Y., Lee, C.H., Aoyama, T., Ichihara, G., Furuhashi, K., Kamijima, M., Gonzalez, F.J., Nakajima, T., 2007. Di(2-ethylhexyl)phthalate induces hepatic tumorigenesis through a peroxisome proliferator-activated receptor alpha-independent pathway. J. Occup. Health 49, 172–182.

Kobayashi, H., Azuma, R., Yasunaga, T., 2009. Expression of excess receptors and negative feedback control of signal pathways are required for rapid activation and prompt cessation of signal transduction. Cell Commun. Signal. 7, 3.

Lee, S.S., Pineau, T., Drago, J., Lee, E.J., Owens, J.W., Kroetz, D.L., Fernandez-Salguero, P.M., Westphal, H., Gonzalez, F.J., 1995. Targeted disruption of the alpha isoform of the peroxisome proliferator-activated receptor gene in mice results in abolishment of the pleiotropic effects of peroxisome proliferators. Mol. Cell. Biol. 15, 3012–3022.

Li, L., Zhang, T., Qin, X.S., Ge, W., Ma, H.G., Sun, L.L., Hou, Z.M., Chen, H., Chen, P., Qin, G.Q., Shen, W., Zhang, X.F., 2014. Exposure to diethylhexyl phthalate (DEHP) results in a heritable modification of imprint genes DNA methylation in mouse oocytes. Mol. Biol. Rep. 41, 1227–1235.

Lovekamp-Swan, T., Davis, B.J., 2003. Mechanisms of phthalate ester toxicity in the female reproductive system. Environ. Health Perspect. 111, 139–145.

Miller, W.L., Auchus, R.J., 2011. The molecular biology, biochemistry, and physiology of human steroidogenesis and its disorders. Endocr. Rev. 32, 81–151.

Qin, X.Y., Zaha, H., Nagano, R., Yoshinaga, J., Yonemoto, J., Sone, H., 2011. Xenoestrogens down-regulate aryl-hydrocarbon receptor nuclear translocator 2 mRNA expression in human breast cancer cells via an estrogen receptor alpha-dependent mechanism. Toxicol. Lett. 206, 152–157.

Schmidt, J.S., Schaedlich, K., Fiandanese, N., Pocar, P., Fischer, B., 2012. Effects of di(2-ethylhexyl) phthalate (DEHP) on female fertility and adipogenesis in C3H/N mice. Environ. Health Perspect. 120, 1123–1129.

Suzuki, Y., Niwa, M., Yoshinaga, J., Mizumoto, Y., Serizawa, S., Shiraishi, H., 2010. Prenatal exposure to phthalate esters and PAHs and birth outcomes. Environ. Int. 36, 699–704.

Suzuki, Y., Yoshinaga, J., Mizumoto, Y., Serizawa, S., Shiraishi, H., 2012. Foetal exposure to phthalate esters and anogenital distance in male newborns. Int. J. Androl. 35, 236–244.

Swan, S.H., 2008. Environmental phthalate exposure in relation to reproductive outcomes and other health endpoints in humans. Environ. Res. 108, 177–184.

Swan, S.H., Main, K.M., Liu, F., Stewart, S.L., Kruse, R.L., Calafat, A.M., Mao, C.S., Redmon, J.B., Ternand, C.L., Sullivan, S., Teague, J.L., 2005. Decrease in anogenital distance among male infants with prenatal phthalate exposure. Environ. Health Perspect. 113, 1056–1061.

Wolf Jr., C., Lambright, C., Mann, P., Price, M., Cooper, R.L., Ostby, J., Gray Jr., L.E., 1999. Administration of potentially antiandrogenic pesticides (procymidone, linuron, iprodione, chlozolinate, p,p'-DDE, and ketoconazole) and toxic substances (dibutyl- and diethylhexyl phthalate, PCB 169, and ethane dimethane sulphonate) during sexual differentiation produces diverse profiles of reproductive malformations in the male rat. Toxicol. Ind. Health 15, 94–118.

Wu, M.T., Wu, C.F., Wu, J.R., Chen, B.H., Chen, E.K., Chao, M.C., Liu, C.K., Ho, C.K., 2012. The public health threat of phthalate-tainted foodstuffs in Taiwan: the policies the government implemented and the lessons we learned. Environ. Int. 44, 75–79.

Zacharewski, T.R., Meek, M.D., Clemons, J.H., Wu, Z.F., Fielden, M.R., Matthews, J.B., 1998. Examination of the in vitro and in vivo estrogenic activities of eight commercial phthalate esters. Toxicol. Sci. 46, 282–293.

Supplemental material to this article can be found at:
http://molpharm.aspetjournals.org/content/suppl/2013/11/21/mol.113.088856.DC1.html

1521-0111/85/2/279–289$25.00
MOLECULAR PHARMACOLOGY
Copyright © 2013 by The American Society for Pharmacology and Experimental Therapeutics
http://dx.doi.org/10.1124/mol.113.088856
Mol Pharmacol 85:279–289, February 2014

MOLECULAR PHARMACOLOGY

Identification of Amino Acid Residues in the Ligand-Binding Domain of the Aryl Hydrocarbon Receptor Causing the Species-Specific Response to Omeprazole: Possible Determinants for Binding Putative Endogenous Ligands[S]

Kazuhiro Shiizaki, Seiichiroh Ohsako, Masanobu Kawanishi, and Takashi Yagi

Division of Cancer Development System, National Cancer Center Research Institute, Tokyo, Japan (K.S.); Division of Environmental Health Sciences, Center for Disease Biology and Integrative Medicine, Graduate School of Medicine, The University of Tokyo, Tokyo, Japan (S.O.); Department of Life Science, Dongguk University, Seoul, Korea (T.Y.); and Department of Biology, Graduate School of Science, Osaka Prefecture University, Osaka, Japan (M.K., T.Y.)

Received July 29, 2013; accepted November 21, 2013

ABSTRACT

Omeprazole (OME) induces the expression of genes encoding drug-metabolizing enzymes, such as CYP1A1, via activation of the aryl hydrocarbon receptor (AhR) both in vivo and in vitro. However, the precise mechanism of OME-mediated AhR activation is still under investigation. While elucidating species-specific susceptibility to dioxin, we found that OME-mediated AhR activation was mammalian species specific. Moreover, we previously reported that OME has inhibitory activity toward CYP1A1 enzymes. From these observations, we speculated that OME-mediated AhR target gene transcription is due to AhR activation by increasing amounts of putative AhR ligands in serum by inhibition of CYP1A1 activity. We compared the amino acid sequences of OME-sensitive rabbit AhR and nonsensitive mouse AhR to identify the residues responsible for the species-specific response. Chimeric AhRs were constructed by exchanging domains between mouse and rabbit AhRs to define the region required for the response to OME. OME-mediated transactivation was observed only with the chimeric AhR that included the ligand-binding domain (LBD) of the rabbit AhR. Site-directed mutagenesis revealed three amino acids (M328, T353, and F367) in the rabbit AhR that were responsible for OME-mediated transactivation. Replacing these residues with those of the mouse AhR abolished the response of the rabbit AhR. In contrast, substitutions of these amino acids with those of the rabbit AhR altered nonsensitive mouse AhR to become sensitive to OME. These results suggest that OME-mediated AhR activation requires a specific structure within LBD that is probably essential for binding with enigmatic endogenous ligands.

Introduction

Omeprazole (OME), a benzimidazole derivative, is a potent suppressor of gastric acid secretion and has been used to treat gastroesophageal reflux disease and duodenal ulcers (Lind et al., 1983). In human hepatoma cells and liver cells, OME is known to induce CYP1A1 and CYP1A2 (Diaz et al., 1990; Curi-Pedrosa et al., 1994; Krusekopf et al., 1997; Yoshinari et al., 2008). The transactivation of these genes is known to be mediated by a ligand-dependent transcriptional factor, aryl hydrocarbon receptor (AhR) and AhR nuclear translocator (Arnt) (Burbach et al., 1992; Reyes et al., 1992). The AhR/Arnt heterodimer binds to the specific nucleic acid sequence known as the xenobiotic response element (XRE), which is located in the 5′-flanking region of CYP1A1 gene and other AhR target genes (Denison et al., 1989). Although it is generally accepted that ligand binding is a key determinant for AhR-mediated transcriptional activity, even in the absence of exogenous ligands (Chang and Puga, 1998; Murray et al., 2005; Shiizaki et al., 2005), some reports have shown that OME induces CYP1A1 expression without binding to AhR using competitive binding assays (Daujat et al., 1992; Dzeletovic et al., 1997). Similar to typical AhR ligands, OME induces translocation of the AhR/Arnt complex to the nucleus, and the complex binds to the XRE of the *Cyp1a1* enhancer region (Quattrochi and Tukey, 1993; Yoshinari et al., 2008). Therefore, OME is considered to activate AhR through a pathway other than ligand binding. Several reports have shown that the protein tyrosine kinase (PTK) pathway is involved in CYP1A1 induction by OME in rat and human hepatoma cells (Backlund et al., 1997; Kikuchi et al., 1998; Lemaire et al., 2004; Backlund and Ingelman-Sundberg, 2005). OME-mediated AhR signaling has been shown

This research was supported by Grants-in-Aid for Scientific Research (S) [Grants 18101002, 18101003]; (C) [Grant 23590162] from MEXT Japan; and in part, by the Environmental Technology Development Fund to S.O. from the Ministry of the Environment.
dx.doi.org/10.1124/mol.113.088856.
[S] This article has supplemental material available at molpharm.aspetjournals.org.

ABBREVIATIONS: AhR, aryl hydrocarbon receptor; Arnt, AhR nuclear translocator; DMEM, Dulbecco's modified Eagle's medium; FBS, fetal bovine serum; FICZ, 6-formylindolo[3,2-*b*]carbazole; ITE, 2-(1*H*-indol-3-ylcarbonyl)-4-thiazolecarboxylic acid methyl ester; LBD, ligand-binding domain; luciferin-CEE, luciferin 6′-chloroethyl ether; 3MC, 3-methylcholanthrene; MEM, minimum essential medium; OME, omeprazole; P450, cytochrome P450; PTK, protein tyrosine kinase; *R*luc, *Renilla* luciferase; TCDD, 2,3,7,8-tetrachlorodibenzo-*p*-dioxin; XRE, xenobiotic response element.

Downloaded from molpharm.aspetjournals.org at ASPET Journals on November 18, 2014

to be attenuated by *c-src* kinase inhibitors or by expression of the dominant negative *c-src* protein. Furthermore, it has been suggested that the tyrosine residue at amino acid position 320 in the human AhR is a putative phosphorylation site required for OME-mediated AhR activation (Backlund and Ingelman-Sundbrg, 2004). However, the molecular mechanisms of OME-mediated AhR activation have not been completely elucidated. In addition, OME-mediated AhR activation has been reported to be species-specific (Kikuchi et al., 1995, Dzeletovic et al., 1997). CYP1A1 induction by OME has been demonstrated in human, but not in mouse, primary hepatocytes and hepatoma cell lines. However, the PTK pathway appears to be unrelated to this interspecies difference because the tyrosine 320 residue is conserved in mouse and human AhRs. By fusing mouse and human hepatoma cells, a gene locus was assigned as a human-specific gene responsible for CYP1A1 induction by OME (Kikuchi et al., 2002). However, specific genes exhibiting response to OME have not been identified. Thus, the mechanism underlying species-specific differences in OME-mediated AhR activation remains unclear. Elucidating such a mechanism could lead to a better understanding of OME-mediated AhR activation.

Recent studies have shown that AhR has physiologic roles such as anti-inflammation and T-cell differentiation (Kimura et al., 2008; Quintana et al., 2008). These discoveries led to suggestions of using AhR ligands for chemotherapy. For example, a selective AhR modulator that exhibits anti-inflammatory properties without XRE-dependent xenobiotic gene expression has been proposed (Murray et al., 2010). Because some AhR ligands are already used in human therapy and because OME-mediated AhR activation is unique, OME and other imidazole compounds may be candidates for selective AhR modulators. Elucidation of the molecular mechanism of OME-mediated AhR activation will be important for such applications.

Recently, a report showed that AhR activation by CYP1A1-inhibiting chemicals is caused by an indirect mechanism involving disruption of the clearance of endogenous ligands (Wincent et al., 2012). We speculated that OME-mediated AhR activation is due to this indirect mechanism because OME is one of the CYP1A1-inhibiting chemicals (Shiizaki et al., 2008). Species-specific response to TCDD (2,3,7,8-tetrachlorodibenzo-*p*-dioxin) is considered to be due to differences in the AhR molecular structure responsible for the ligand binding affinity (Bohonowych and Denison, 2007), although this topic is controversial. If a putative ligand is related to OME-mediated AhR activation, a species-specific OME response would be generated because of the affinity of the putative ligand conferred by the AhR structure, as well as response to TCDD. In addition, the structural differences in AhR will be due to particular amino acid residues.

In this study, we used AhRs derived from various laboratory animals and humans to demonstrate that species-specific activation by OME depends on specific amino acids within the AhR amino acid sequences.

Materials and Methods

Chemicals. Omeprazole, 3-methylcholanthrene (3MC), ellipticine, kynurenic acid, and 2-(1*H*-indol-3-ylcarbonyl)-4-thiazolecarboxylic acid methyl ester (ITE) were purchased from Sigma-Aldrich (St. Louis, MO). TCDD (>99.5% purity) was obtained from Cambridge Isotope Laboratories (Andover, MA). β-Naphthoflavone was purchased from Wako Pure Chemical (Osaka, Japan). Indirubin was provided by Dr. Tomonari Matsuda (Kyoto University, Kyoto, Japan). FICZ (6-formylindolo[3,2-*b*]carbazole) was purchased from Biomol International LP (Plymouth Meeting, PA). All chemicals were dissolved in dimethylsulfoxide and added to media. The final concentration of dimethylsulfoxide was adjusted to 0.1% (v/v) in culture media.

CYP1A1 Activity Determined by Cytochrome P450-Glo Assays. CYP1A1 activity was determined using a cytochrome P450 (P450)-Glo CYP1A1 Assay (Promega, Madison, WI) according to the manufacturer's instructions. Sf9 cell microsomes containing recombinant human CYP1A1 were purchased from Becton Dickinson (Franklin Lakes, NJ). In brief, an aliquot (0.5 pmol) of microsomes was mixed with 100 mM KPO_4 buffer (25 μl) containing 120 μM of luciferin 6′-chloroethyl ether (luciferin-CEE). Then, OME (final concentration 0.5–100 μM) or ellipticine (final concentration 0.1–10 μM) was added to reaction cocktails and incubated at 37°C for 10 minutes. After preincubation, 25 μl of 2× NADPH-regenerating system solution (2.6 mM $NADP^+$, 6.6 mM glucose-6-phosphate, 0.4 U/ml glucose-6-phosphate dehydrogenase, and 6.6 mM $MgCl_2$) was added and incubated at 37°C for 30 minutes. Luciferin obtained after conversion of luciferin-CEE by CYP1A1 was detected by adding the Luciferin Detection Reagent included in the assay kit, and luminescence was detected using the Wallac Arvo SX Multi-Label counter (PerkinElmer, Boston, MA).

Plasmid Construction. The reporter plasmid pX4TK-Luc, which includes the firefly luciferase gene under the control of four copies of XRE and the thymidine kinase promoter, was a gift from K. Sogawa (Tohoku University, Sendai, Japan). The expression plasmids containing AhR cDNAs from six mammalian species were constructed as follows. cDNAs were prepared from mouse (*Mus musculus*, strain C57BL), human (*Homo sapiens*), rat (*Rattus norvegicus*, Holtzman), rabbit (*Oryctolagus cuniculus*, New Zealand White), hamster (*Mesocricetus auratus*, Syrian), and guinea pig (*Cavia porcellus*, Hartley). The open reading frames of each AhR were amplified by reverse-transcription polymerase chain reaction and inserted into the MluI and XhoI sites of the pCI-neo vector (Clontech, Palo Alto, CA). To construct the chimeric mouse/rabbit AhRs, AhR cDNA fragments based on the mouse and rabbit AhR ligand-binding domains (LBDs) (Fukunaga et al., 1995) were individually amplified, joined by overlapping polymerase chain reaction, and subcloned into the pCI-neo vector. Single point mutations were generated using a QuikChange Site-Directed Mutagenesis Kit (Stratagene, La Jolla, CA). All primers used in this study are shown in Supplemental Table 1.

Cell Cultures and Transfection. The human epithelial carcinoma cell line HeLa and murine hepatoma cell lines Hepa1c1c and its derivative c12 were obtained from the American Type Culture Collection (Rockville, MD). HeLa cells were grown in minimum essential medium (MEM) containing 10% charcoal-stripped fetal bovine serum (FBS) and 1× Antibiotic-Antimycotic (Invitrogen, Carlsbad, CA). Hepa1c1c and c12 cells were grown in Dulbecco's modified Eagle's medium (DMEM) containing 10% charcoal-stripped FBS and 1× Antibiotic-Antimycotic. All cultures were incubated at 37°C in 5% CO_2. Transfection was performed by a liposome method. In brief, 1 μg of plasmid DNA and 4 μl of Plus reagent (Invitrogen) were combined in 200 μl of OPTI-MEM (Invitrogen). After incubation for 15 minutes, 2 μl of Lipofectamine reagent (Invitrogen), diluted with 200 μl OPTI-MEM, was added. The cells were plated in six-well tissue culture plates at 30%–40% confluence a day before transfection. Liposomes were added in serum-free medium for 3 hours and then replaced with MEM or DMEM containing 10% charcoal-stripped FBS without 1× Antibiotic-Antimycotic.

Luciferase Assay. The effects of OME and typical AhR agonists on XRE-dependent transcriptional activity were evaluated by cotransfecting the AhR expression plasmid, the reporter plasmid pX4TK-Luc (Mimura et al., 1999), and the *Renilla* luciferase (*R*luc) expression vector pRL-CMV (Promega) into cells. The transfected cells were washed with cold phosphate-buffered saline and lysed in 25 μl of 1× passive lysis buffer (Promega). Aliquots (10 μl) of the

Downloaded from molpharm.aspetjournals.org at ASPET Journals on November 18, 2014

lysates were transferred to 96-well plates, and Luc$^+$ and *R*luc luminescence was measured using the Dual-Luciferase Reporter Assay System (Promega) in the Wallac Arvo SX Multi-Label counter. Transfection and translation efficiencies varied between independent experiments, and the results were normalized by calculating Luc$^+$/*R*luc ratios. All assays were performed in triplicate.

Immunoblotting. Immunoblotting was performed to evaluate expressed AhR protein levels after transient transfection experiments. Cells plated in six-well plates were washed with phosphate-buffered saline, lysed in 0.5 ml of SDS lysis buffer (1% SDS, 10 mM EDTA, and 50 mM Tris-HCl, pH 8) containing Complete Protease Inhibitor Cocktail (Roche, Basel, Switzerland) and sonicated to shear DNA. Protein concentration in the cell lysates was measured by the Bradford method using a Bio-Rad Protein Assay (Bio-Rad Laboratories, Munich, Germany), and 20-μg aliquot of each sample was separated on an SDS-polyacrylamide gel. Immunoblotting for AhR was performed as described previously (Pollenz et al., 1994) with anti-human AhR antibody (SA-210; Biomol GmbH, Hamburg, Germany). Detection was performed with peroxidase-labeled anti-rabbit antibody using the ECL Plus detection system (GE Healthcare Bio-Sciences, Uppsala, Sweden). The bands were visualized and imaged using ChemiDoc XRS Plus (Bio-Rad Laboratories).

Generation of Stable Cell Lines Expressing Mutant AhRs. The pCI-neo plasmids containing mouse and rabbit AhR cDNAs with point mutations were transfected into c12 cells. Stable transformants expressing AhRs were selected by using G418 and screened for ethoxyresorufin-*O*-deethylase activity as described previously (Kennedy and Jones, 1994) after treatment with 10 nM TCDD. We chose and mixed more than six representative clones from transformants obtained with each plasmid and investigated CYP1A1 inducibility by TCDD and OME using real-time reverse-transcription polymerase chain reaction methods. In brief, the cells plated in six-well plates at 80% confluence were exposed to 50 μM OME or 10 nM TCDD. After 12 hours of exposure, total RNA was isolated using Isogen (Nippon Gene, Tokyo, Japan) according to the manufacturer's instructions. An aliquot (2 μg) of total RNA was subjected to RT using MultiScribe RT (Applied Biosystems, Foster City, CA) and oligo-dT primers. An aliquot of cDNA (2 μl) or calibrator plasmid DNA (pCI-neo-mAhR) was amplified with master mixture (SYBR Premix Ex Taq; Takara Bio, Kyoto, Japan) containing gene-specific primers. The primer pair for mouse CYP1A1 cDNA amplification is shown in Supplemental Table 1. The reaction mixture was amplified using the Smart Cycler System (Cepheid; Takara Bio) under the following conditions: an initial incubation at 95°C for 15 minutes, followed by 40 cycles of 95°C for 15 seconds, 60°C for 20 seconds, and 72°C for 10 seconds. To confirm amplification specificity, the PCR products were subjected to melting curve analyses. A calibration curve was generated by threshold

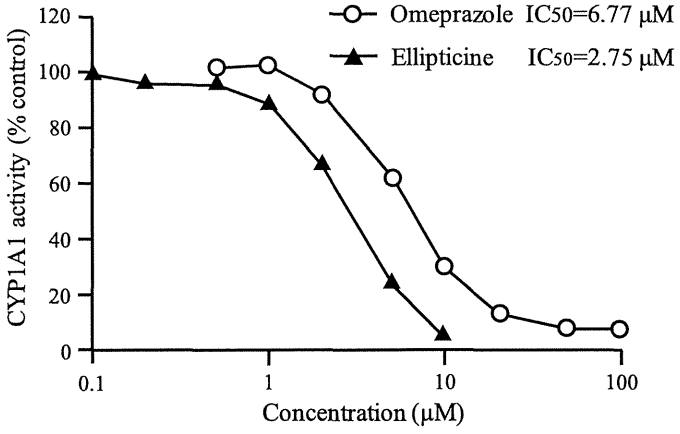

Fig. 1. Inhibition of human CYP1A1 activity by omeprazole. CYP1A1 activity was determined using P450-Glo Assays and Sf9 cell microsomes containing recombinant human CYP1A1. Luciferin-CEE (a specific substrate for CYP1A1) and microsomes were incubated at 37°C for 30 minutes with various concentrations of omeprazole or ellipticine. Each data point represents the mean of duplicate determinations.

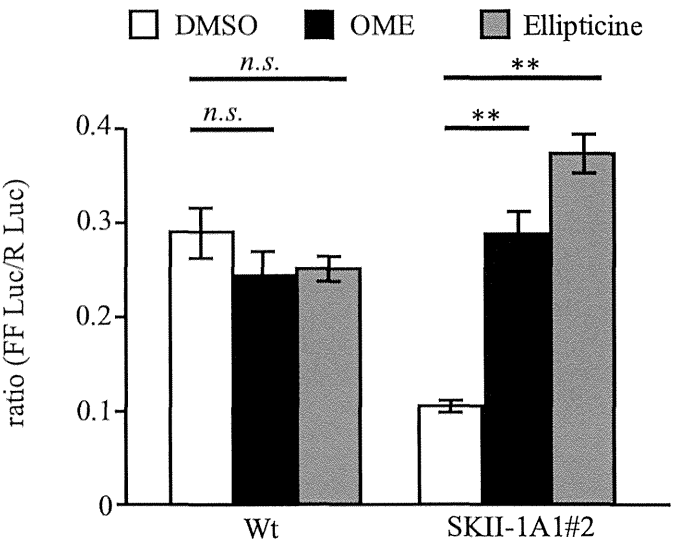

Fig. 2. OME restores XRE-dependent transcription in CYP1A1-overexpressing SKII-1A1 cells and CYP1A1-deficient SK-Hep-1 cells. CYP1A1-deficient SK-Hep-1 (Wt) and its derivative cell lines overexpressing CYP1A1 (SKII-1A1#2) cultured in medium containing 10% FBS were transfected with the 4xXRE-Luc reporter gene and pCMV-Rluc. After transfection, fresh medium containing 100 μM omeprazole (closed column), 5 μM ellipticine (gray column) or dimethylsulfoxide (DMSO) (solvent control, open column) was added. Data are represented as the ratio of firefly luciferase activity to *Renilla* luciferase activity observed 16 hours after OME was added. (FFluc/*R*luc, mean ± S.D., $n = 3$) (**$P < 0.01$, n.s., no significant difference to control). FFluc, firefly luciferase.

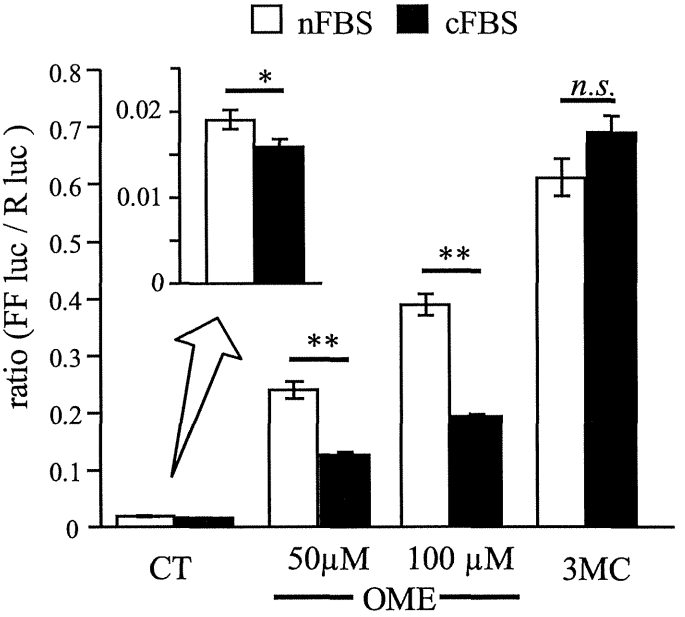

Fig. 3. Effects of FBS on XRE-dependent transcriptional activation. HepG2 cells were transfected with the 4xXRE-Luc reporter gene and pCMV-Rluc. After transfection, the culture medium was changed to fresh DMEM containing normal FBS (nFBS, open column) or charcoal-stripped FBS (cFBS, closed column). Twenty-four hours after medium exchange, dimethylsulfoxide (solvent control; CT), 50 or 100 μM OME was added. Significant reductions in OME-induced transcription was noted with charcoal stripping; however, 3MC (1 μM)-induced transcription was not affected. Data are represented as mean ± S.D. ($n = 3$) 16 hours after OME addition. (*$P < 0.05$; **$P < 0.01$; n.s., no significant difference). FFluc, firefly luciferase.

Downloaded from molpharm.aspetjournals.org at ASPET Journals on November 18, 2014

cycles of calibrators of a known plasmid copy number. The initial quantity of target mRNA in the samples was determined by correlating their threshold cycles to the calibration curve.

Results

OME Inhibits CYP1A1 Activity. To examine whether OME directly inhibits CYP1A1 activity, recombinant human CYP1A1 proteins expressed by Sf9 cells were used in the inhibition study. In addition to ellipticine, a typical CYP1A1 inhibitor, OME also inhibited CYP1A1 activity. The mean inhibitory concentration value was 6.77 μM in case of OME and 2.75 μM in ellipticine (Fig. 1, data re-examined as reported in our previous study, Shiizaki et al., 2008). CYP1A1 activity was inhibited nearly 90% by more than 20 μM of OME, and this concentration correlated to the concentration of OME required for AhR activation (Diaz et al., 1990; Dzeletovic et al., 1997).

We confirmed species-specific induction of CYP1A1 by OME (Supplemental Fig. 1A). Induction of CYP1A1 mRNA by OME occurred not only in human hepatoma HepG2 cells but also in mouse Hepa1c1c cells (Kikuchi et al., 1995). This induction was well correlated with XRE-driven reporter gene induction (Supplemental Fig. 1B). We used this reporter assay system to evaluate OME-mediated AhR activation, which, consequently, led to CYP1A1 induction.

OME Restores XRE-Dependent Transcription in CYP1A1-Overexpressing SKII-1A1 Cells and CYP1A1-Deficient SK-Hep-1 Cells. As reported in our previous study, in the presence of 10% FBS, the human hepatoma cell line SK-Hep-1, which is deficient in *CYP1A1* expression, showed higher basal transcription from the XRE-driven reporter gene without additional exogenous ligands than other human hepatoma cells (Shiizaki et al., 2005). We compared basal transcription levels of CYP1A1-overexpressing cell lines (SKII-1A1 cells) and found that basal transcription levels in these cells were significantly lower than those in wild-type SK-Hep-1 cells. Using this reporter system, OME or ellipticine was added to culture media of the wild-type SK-Hep-1 and SKII-1A1#2 cells (one of the CYP1A1-overexpressing clones). OME restored the transcription in the SKII-1A1#2 cells to a level similar to that in the wild-type cells (Fig. 2). Treatment of CYP1A1 inhibitor ellipticine indicated similar results. These observations suggest that OME does not transactivate XRE-driven reporter genes directly via AhR activation but instead inhibits transcription repression by CYP1A1 activity.

Charcoal-Stripping of Serum Diminished the Basal Transcription Level and OME-Induced Transcription of the XRE-Driven Reporter Gene in HepG2 Cells. Next, we tested the effect of FBS on the transcription induction of XRE-driven reporter genes by OME to provide indirect evidence of the presence of substances in FBS that might transactivate AhR. The human hepatoma cell line HepG2 and SK-Hep-1 cells are similar in terms of the expression levels of AhR and Arnt molecules (Shiizaki et al., 2005). The 4xXRE-Luc reporter gene and pCMV-Rluc were cotransfected into HepG2 cells. After transfection, the culture medium was changed to fresh DMEM containing normal FBS or charcoal-stripped FBS. Although OME-induced transcription was clearly observed in DMEM containing normal FBS, significantly less OME-induced transcription was observed in DMEM containing charcoal-stripped FBS (Fig. 3). Charcoal-stripping of FBS did not reduce 3MC (1 μM)-induced transcription. Together with this and the previously mentioned results (Figs. 1 and 2), it is highly suspected that OME-mediated AhR activation of the XRE-dependent gene is due to the inhibition of the activity of CYP1A1 enzymes, which may metabolize putative AhR ligands contained in FBS.

Comparison of the Responses of AhRs Derived from Various Mammals to OME. While exploring the genes that cause species-specific susceptibility against dioxin, we prepared six AhR expression plasmids from six mammalian species using pCI-neo vectors. In these experiments, we used HeLa cells, which possess *CYP1A1* and express a similar level of ARNT molecules and a lower level of AhR molecules compared with HepG2 or SK-Hep-1 cells. We also used mouse

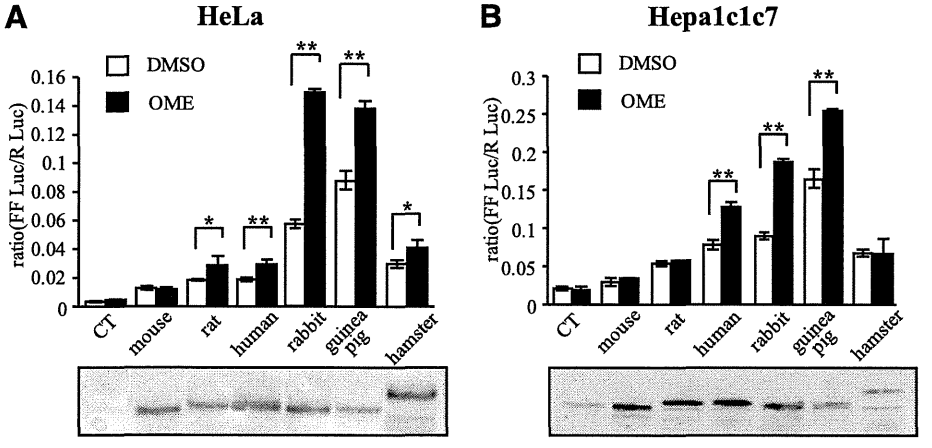

Fig. 4. Comparison of the induction of XRE-dependent transcription by OME through six mammalian AhR species. HeLa (A) and Hepa1c1c (B) cells were transfected with an empty vector (pCI-neo, CT, negative control) or six mammalian AhR expression plasmids (generated from the mouse, rat, human, rabbit, guinea pig, and hamster) together with the XRE-driven pX4TK-Luc reporter gene and pCMV-Rluc. After 24 hours, the cells were exposed to 100 μM OME or 0.1% dimethylsulfoxide (DMSO). After 16 hours of incubation, the cells were lysed, and firefly luciferase and *Renilla* luciferase activities were measured. Data represent the mean ± S.D. of normalized firefly luciferase (FFluc)/*Renilla* luciferase activities of three independent experiments. OME-treated groups (closed columns) were compared with DMSO controls (open columns) using one- or two-way analysis of variance, and statistically significant differences are denoted by asterisks ($*P < 0.05$; $**P < 0.01$). Total cell lysates were subjected to immunoblotting to confirm the expression level of each AhR (lower panels).

Downloaded from molpharm.aspetjournals.org at ASPET Journals on November 18, 2014

hepatoma Hepa1c1c7 cells, which expressed a sufficient level of AhR. During this project, we used OME in addition to TCDD to examine the species-specific influence on AhR-dependent transcription. XRE-driven reporter gene assays were performed by cotransfection of the previously mentioned six AhR expression vectors and 4xXRE-Luc reporter genes.

The constitutive transcription of XRE-dependent luciferase differed among AhR species expressed in HeLa and Hepa1c1c7 cells (Fig. 4, A and B). Although overexpressed AhR protein levels were almost similar in HeLa cell experiments, the highest basal transcription level was detected in the guinea pig AhR, followed by the rabbit AhR (Fig. 4A). The pattern of basal transcription levels with each AhR in the Hepa1c1c7 cell experiments was similar to those in the HeLa cells; however, the levels did not correlate with the protein levels measured by immunoblotting (Fig. 4B). Of the six AhRs, the mouse AhR transfection caused the least increment in constitutive activity in both cells, as well as no significant induction of genes with the addition of OME (Fig. 4, A and B). Considering the effects of exogenous AhRs transfection, reporter gene induction by OME was highest when the rabbit AhR was used, followed by the guinea pig AhR (Fig. 4, A and B). However, in addition to the mouse AhR, rat and hamster AhRs were not activated by OME in mouse hepatoma cells. These results suggest that transcriptional activation by OME was dependent on the AhR species as well as the species of host cells.

Responses of Chimeric AhRs to OME. According to our already described observations, we speculated that the rabbit AhR must contain a domain responsible for OME-induced XRE-dependent transcription. Six chimeric AhRs were constructed using mouse and rabbit AhR cDNAs (Fig. 5A). Among the chimeric constructs, MR1, RM2, and MRM1, which included the rabbit LBD (amino acids 261–393), showed OME-dependent reporter gene induction. MR2, RM1, and RMR1, which included the mouse LBD (amino acids 257–389), did not respond to OME, despite the other regions of these chimeras were of the rabbit AhR (Fig. 5A). To determine the minimum requirement for the response to OME, chimeric AhRs were constructed with half LBDs; however, no constructs with partial rabbit AhR LBDs responded to OME (Fig. 5B). These data suggest that the response to OME required the complete rabbit AhR LBD and that multiple amino acid combinations specific to the rabbit AhR should be indispensable for OME-mediated AhR activation.

Determination of the Amino Acid Residues Responsible for OME-Mediated AhR Activation. Next, we conducted a study of a single amino acid substitution in the rabbit AhR that would eliminate OME-mediated AhR activation. There are 16 amino acid differences between the rabbit and mouse AhR LBDs (Fig. 6A). As shown in Fig. 6B, the basal transcriptional activity of rabbit AhR mutants was variously changed by a single amino acid substitution. Most of the mutants, except M328I, T353A, and F367L, did not much influence the OME-mediated transcriptional level. These three mutants reduced induction to less than one half of wild-type rabbit AhR, which showed an approximately 3-fold change by OME. The OME-mediated inductive ratio of M328I, T353A, and F367L was 1.7-, 1.2-, and 1.0-fold, respectively. Difference in properties between mouse AhR and rabbit AhR is the basal transcriptional activity and OME-induced transcriptional activity. By plotting these properties to emphasize differences of AhR mutants, we found the three mutant AhRs—M328I, T353A, and F367L—indicated intermediate properties of the mouse AhR and rabbit AhR (Fig. 6C).

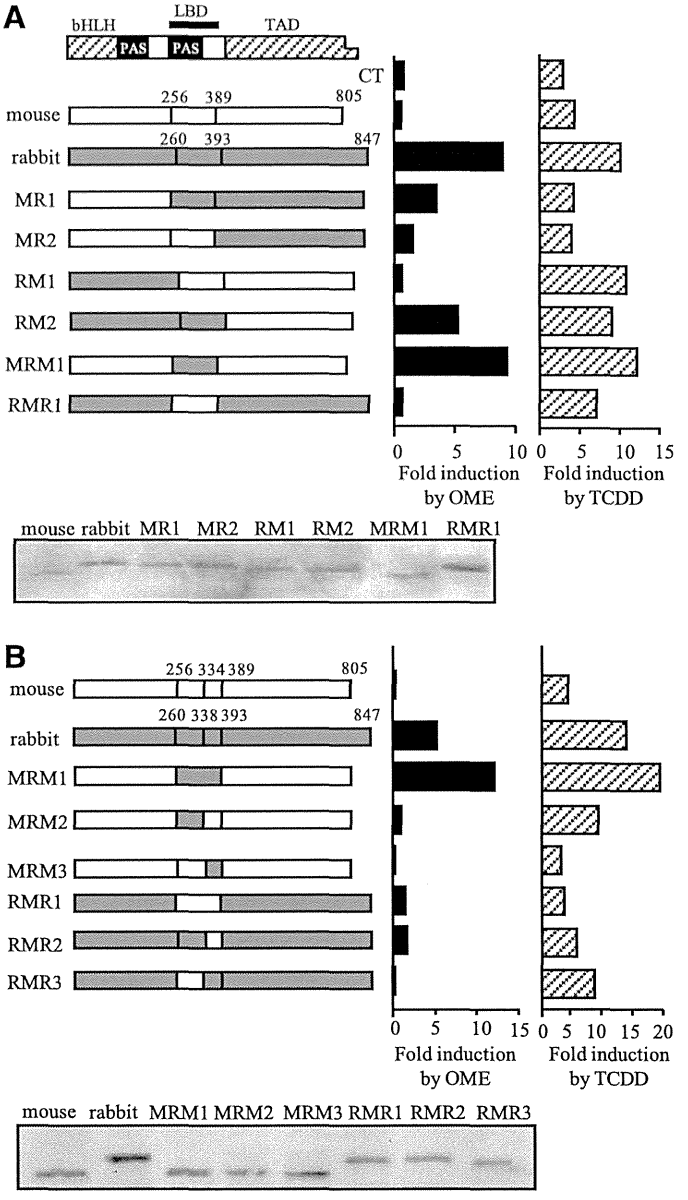

Fig. 5. Construction of chimeric AhRs and their responses to OME and TCDD. (A) Schematic diagrams of the six chimeric constructs (MR1, MR2, RM1, RM2, MRM1, and RMR1) generated from parts of cDNAs of the rabbit (white) and mouse AhRs (gray) for the first screening. HeLa cells were transfected with expression plasmids containing chimeric AhRs or the empty vector (CT, negative control) together with pX4TK-Luc and exposed to 100 μM OME, 10 nM TCDD, or 0.1% dimethylsulfoxide (DMSO). Induction of the reporter gene by these chimeric AhRs after exposure to OME (left) and TCDD (right). Data represent means of the fold induction above the control from two independent experiments. Immunoblotting was performed to confirm the expression level of each AhR (lower panel). (B) The second screening to narrow the responsible domain. Four more chimeric constructs (MRM2, MRM3, RMR2, and RMR3) were generated and subjected to the same assay. Immunoblotting was performed to confirm the expression level of each AhR (lower panel).

In addition, we constructed double and triple substitutions of these three amino acid residues in the rabbit AhR. As shown in Fig. 7A, the combinations of M328I and T353A or

Downloaded from molpharm.aspetjournals.org at ASPET Journals on November 18, 2014

A

```
Mouse  257 LALFAIATPLQPPSILEIRTKNFIFRTKHKLDFT 290
Rabbit 261 ********************************** 294

Mouse  291 PIGCDAKGQLILGYTEVELCTRGSGYQFIHAADI 324
Rabbit 295 *T*******IV*****A***M***********M 328

Mouse  325 LHCAESHIRMIKTGESGMTVFRLLAKHSRWRWVQ 358
Rabbit 329 *Y***************LA*****T*DN**A*** 362

Mouse  359 SNARLIYRNGRPDYIIATQRPLTDEEGREHL    389
Rabbit 363 ****F**K*****F****************    393
```

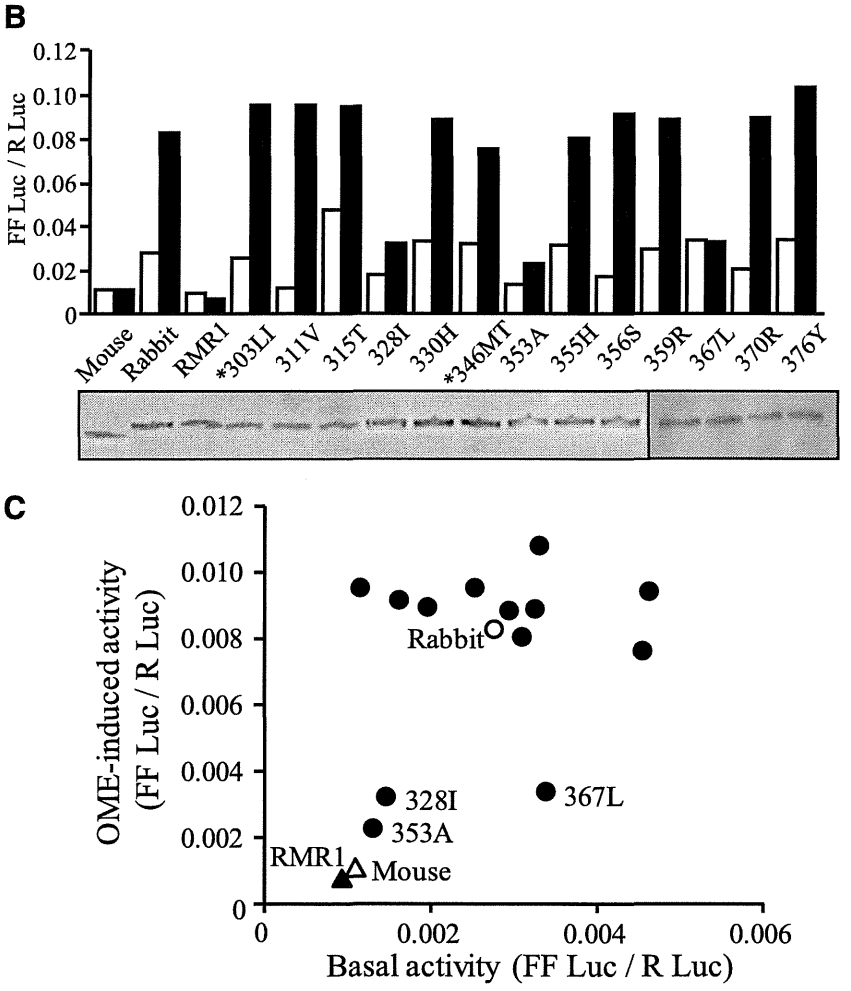

Fig. 6. Effects of point mutations on the response of the rabbit AhR to OME. (A) Amino acid alignment of mouse and rabbit AhR LBDs. Identical amino acid residues are indicated by asterisks. Differing amino acids are indicated in bold. Underlined sequences indicate the overlapping sequence for connecting with the mouse and rabbit LBDs shown in Fig. 5B. (B) Amino acids within the rabbit AhR LBD were individually replaced with the corresponding amino acids of the mouse AhR. RMR1 is the construct as shown in Fig. 5A. Asterisks indicate the mutated AhR in which two adjacent amino acids were replaced simultaneously. HeLa cells were transfected with expression plasmids containing mutated AhRs, pX4TK-Luc, and pCMV-Rluc. After 24 hours, the cells were exposed to 100 μM OME or 0.01% dimethylsulfoxide (DMSO) for 16 hours. Data represent the means of normalized firefly luciferase/*Renilla* luciferase activities of two independent experiments. Total cell lysates were prepared 24 hours after transfection and analyzed using immunoblotting to confirm the expression level of each AhR (lower panels). (C) The relationship between basal transcriptional activity and the OME-mediated transcriptional activity were plotted. ○, wild-type rabbit AhR; ●, rabbit AhR mutants; △, wild-type mouse AhR; ▲, RMR1 chimera AhR.

T353A and F367L substitutions impaired OME-mediated transcriptional induction. Moreover, the triple substitutions of M328I, T353A, and F367L exhibited properties that were remarkably similar to those of the mouse AhR (i.e., low constitutive activity and OME unresponsiveness). In contrast, mouse AhRs with single amino acid substitutions of I324M, A349T, or L363F, which are residues equivalent to M328, T353, and F367 in the rabbit AhR, slightly introduced OME responsiveness with increased levels of constitutive activities (Fig. 7B). However, triple substitutions of these three residues in the mouse AhR resulted in an approximately 5-fold induction by OME, which was not observed in wild-type mice.

Among the three amino acids, we focused on rabbit F367 because this residue is rabbit-specific (Fig. 8A). In addition, the guinea pig AhR was as responsive to OME as the rabbit AhR, and the amino acid corresponding to rabbit F367 is V368 in the guinea pig AhR, which is different in the other four species (Leu). Therefore, we constructed several mutated mouse and guinea pig AhRs to confirm that Val in this position was effective for the response to OME. As shown in Fig. 8B, the mouse AhR with triple substitutions of L363V, I324M, and A349T responded more to OME compared with double substitutions of I324M and A349T. In contrast, the response of the guinea pig AhR to OME was abolished by the V368L substitution. These results suggest that the combination of three amino acid residues of the AhR (i.e., Met, Thr, and Phe) are required for the response to OME) and also that Phe can be replaced with Val. The importance of these three amino acid residues in the OME response was confirmed by human AhR mutants as well as guinea pig AhR (Supplemental

Downloaded from molpharm.aspetjournals.org at ASPET Journals on November 18, 2014

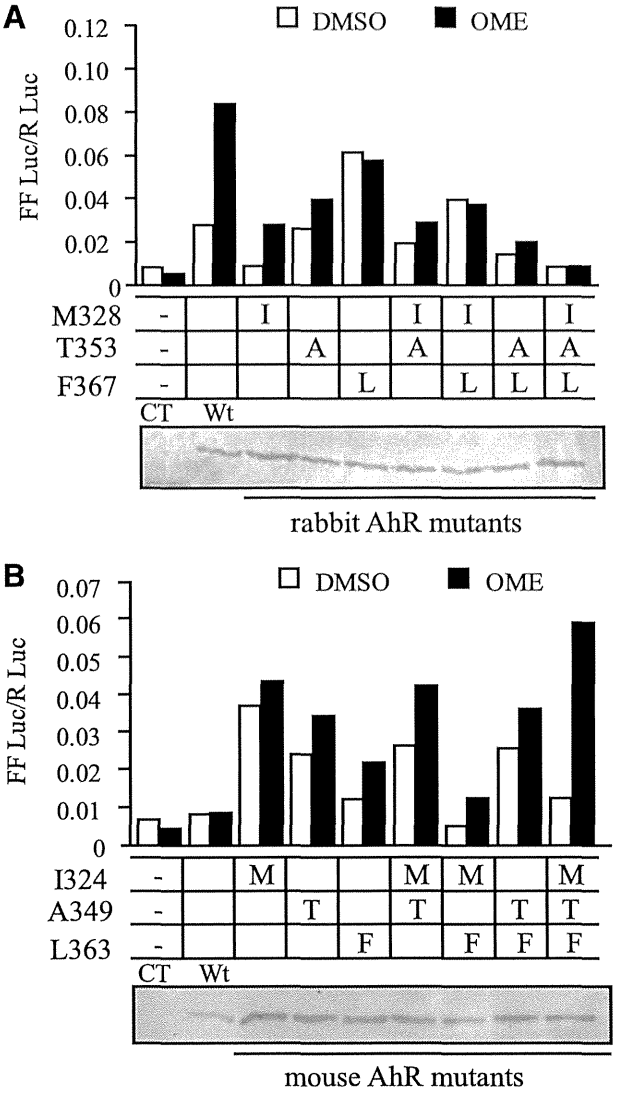

Fig. 7. Effect of single, double, and triple mutations on the response of rabbit and mouse AhRs to OME. (A) Rabbit AhRs with combinations of the three mutations of M328I, T353A, and F367L were transfected into HeLa cells along with the reporter genes. The combinations of the three mutations are indicated in the bottom table of the graph. I, 328Ile; A, 353Ala; L, 367Leu; CT, empty expression vector; Wt, wild-type rabbit AhR. The cells were exposed to 100 μM OME or 0.01% dimethylsulfoxide (DMSO) for 16 hours. Data represent the means of normalized firefly luciferase (FFluc)/*Renilla* luciferase activities of two independent experiments. (B) Mouse AhRs with combinations of the three mutations of I324M, A349T, and L363F were prepared, and luciferase assays were performed as described above. The combinations of the three mutations are indicated in the bottom table of the graph. M, 324Met; T, 349Thr; F, 363Phe; Wt, wild-type mouse AhR. Total cell lysates were prepared 24 hours after transfection and analyzed using immunoblotting to confirm the expression level of each AhR (lower panels).

Fig. 2). When two amino acid residues (330M and 355T) in human AhR were changed to mouse-type amino acid (330I and 355A), OME response was attenuated. Contrary to this, 369F, which is particularly in rabbit AhR, represent higher OME-response than wild-type human AhR.

CYP1A1 Gene Induction by OME Restored the Three Amino Acid Substitutions in the Mouse AhR and Abolished Them in the Rabbit AhR. To confirm the results that M328, T353, and F367 in the rabbit AhR are responsible for the OME-mediated AhR activation, we established cell lines that stably expressed AhRs, including the triple point mutations. The c12 cell line, which is a Hepa1c1c-derived subline lacking endogenous AhR expression, was used for this purpose and examined for CYP1A1 induction by TCDD or OME exposure. As shown in Fig. 9, CYP1A1 mRNA induction by OME was similar to that observed in the reporter assays (Fig. 7); that is, the induction was limited to the cells expressing the wild-type rabbit AhR or the mouse AhR with the three amino acid substitutions. TCDD-induced CYP1A1 mRNA induction was observed at similar levels in all cell lines expressing both wild-type and mutated AhRs, suggesting that TCDD-induced AhR activation was not influenced by these amino acid substitutions.

Responses of Mutated AhRs to Typical AhR Ligands. Next, we characterized the responses of the mutated AhRs to typical AhR ligands, including AhRs with substitutions of the three amino acids involved in the response to OME. As shown in Fig. 10 and Table 1, EC_{50} values calculated from the dose-response curves of three typical chemical ligands were slightly changed (within 2-fold) by these three amino acid substitutions that drastically reversed OME responsiveness. We also tested candidates for endogenous ligands, namely, ITE (Song et al., 2002), FICZ (Wei et al., 1998), indirubin (Adachi et al., 2001), and kynurenic acid (DiNatale et al., 2010), which have induction potencies that differ between mouse and rabbit AhRs. FICZ induced transcriptional activity at a lower concentration with the rabbit AhR than with the mouse AhR, whereas indirubin had a reverse effect. However, as with the chemical ligands, the dose-response curves and EC_{50} values for the putative endogenous ligands were not much changed by the three amino acid substitutions. (Fig. 11; Table 1). These results show that these three amino acid residues define OME sensitivity but do not influence the responsiveness of the other AhR ligands tested in this study.

Discussion

This study aimed to identify and experimentally validate the factor(s) generating species-specific responsiveness of AhR to OME. First, we speculated that OME-mediated AhR activation is due to increasing amounts of putative AhR ligands resulting from the inhibition of CYP1A1 activity by OME. This hypothesis is based on the following observations: 1) OME-mediated AhR activation required CYP1A1 activity and was influenced by endogenous ligands included in serum. 2) The concentration of OME activating AhR was higher than with that of the typical AhR ligand and was similar to the concentration of OME required for CYP1A1 inhibition. 3) The comparison of AhRs from six mammalian species revealed that transcriptional activation of the reporter gene by OME seemed to correlate with the basal transcription level, reflecting the response of the putative endogenous ligand. If a type of ligand mediates OME-dependent AhR activation, OME responsiveness would be attributable to the AhR itself, independent of host cells. In the present study, we constructed chimeric AhRs from mouse and rabbit AhRs, which indicated that OME responsiveness required multiple amino acid residues present in the LBD of the rabbit AhR. These amino acid residues were not present in the mouse AhR. In conclusion, we demonstrated that M328, T353, and F367 of the rabbit AhR were required for OME responsiveness.

These results are fundamentally different from those of previous reports on cell-specific factors that define OME

Downloaded from molpharm.aspetjournals.org at ASPET Journals on November 18, 2014

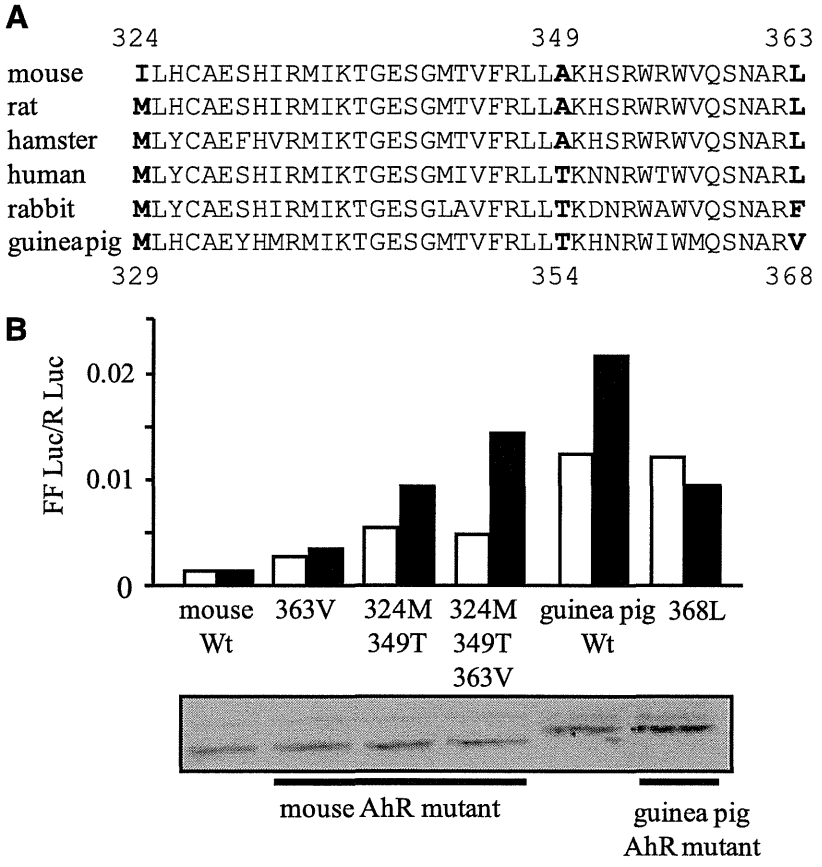

Fig. 8. Effect of single, double, and triple mutations on the response of mouse and guinea pig AhRs to OME. (A) Alignment of the LBD amino acid sequences for six mammalian AhRs. The numbers indicate the amino acid positions in the mouse AhR (top line) and guinea pig AhR (bottom line). The three candidate amino acids that are crucial for the response to OME are in bold font. (B) Mouse AhRs with combinations of the three mutations and the guinea pig AhR with the V368L substitution were transfected into HeLa cells along with the reporter genes. Wt, wild-type mouse AhR or wild-type guinea pig AhR. The cells were exposed to 0.01% dimethylsulfoxide (DMSO) or 100 μM OME for 16 hours. Data represent the means of normalized firefly luciferase (FFluc)/*Renilla* luciferase activities of two independent experiments. Total cell lysates were prepared 24 hours after transfection and analyzed using immunoblotting to confirm the expression level of each AhR (lower panel).

responsiveness (Kikuchi et al., 1995, 2002; Dzeletovic et al., 1997). Some of the differences may be due to the species used because most of the mentioned studies used the human AhR, whereas we primarily used the rabbit AhR, which is highly sensitive to OME. In a previous report (Dzeletovic et al., 1997), the human AhR transiently expressed in mouse hepatoma c12 cells was not activated by OME. We performed a similar experiment with c12 cells stably expressing the rabbit AhR, and these cells exhibited inducible expression of CYP1A1 by OME (Fig. 9). We thought the stably expressed rabbit AhR altered intracellular conditions (e.g., the basal level of CYP1A1 expression) to respond to the AhR activator. In fact, the c12-derived cells expressing the rabbit AhR exhibited a raised level of constitutive CYP1A1 expression and remarkable CYP1A1 induction (>15-fold) on TCDD exposure.

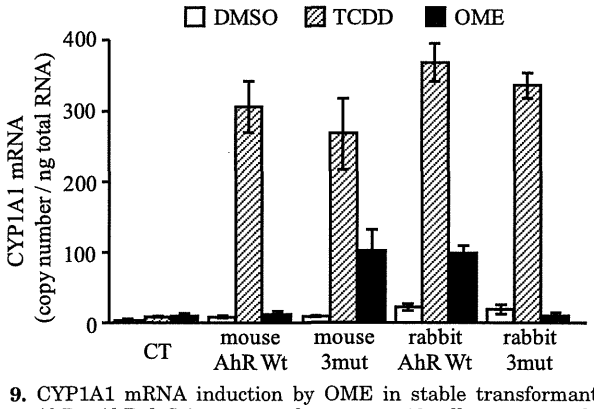

Fig. 9. CYP1A1 mRNA induction by OME in stable transformants of mutant AhRs. AhR-deficient mouse hepatoma c12 cells were transfected with the expression vector of the mouse AhR, rabbit AhR, their derivative mutated AhRs. Mouse 3mut, mouse AhR with I324M, A349T, and L363F substitutions or pCI-neo empty vector (CT, negative control). Rabbit 3mut, rabbit AhR with M328I, T353A, and F367L substitutions. After transfection, a heterogeneous population of G418-resistant cells was maintained and exposed to 0.1% dimethylsulfoxide (DMSO) (solvent control), 10 nM TCDD, or 100 μM OME. After 16 hours of incubation, total RNA was isolated, and mouse CYP1A1 mRNA was measured using real-time reverse-transcription polymerase chain reaction as described in *Materials and Methods*. Data represent mean ± S.D. (n = 3).

Several investigations have identified specific amino acid residues that are important for AhR activation. We previously reported that L318 in the mouse AhR is required for the response to β-naphthoflavone (Goryo et al., 2007). An AhR polymorphism (A375V) in C57BL/6 and DBA/2 mice results in a difference in TCDD binding affinity and consequent toxicity (Ema et al., 1994). Two polymorphisms, V325I and A381S, in the common tern and chicken AhRs are responsible for sensitivity to TCDD (Karchner et al., 2006). Interestingly, the V325I polymorphism in the bird species corresponds to the mouse AhR I324, one of the critical amino acids for OME responsiveness. In the tern AhR, Ile is required in this position for high sensitivity to TCDD. The single mutation I324M in the mouse AhR was insufficient for producing a response to OME but instead increased basal transcriptional activity. The amino acid residue at this position could be close to TCDD and may be one of the key amino acids for ligand binding and constitutive activity. As mentioned in *Results*, F367 is specific to the rabbit AhR. In the guinea pig AhR, the corresponding amino acid is V363, and the L363V substitution was an

Downloaded from molpharm.aspetjournals.org at ASPET Journals on November 18, 2014

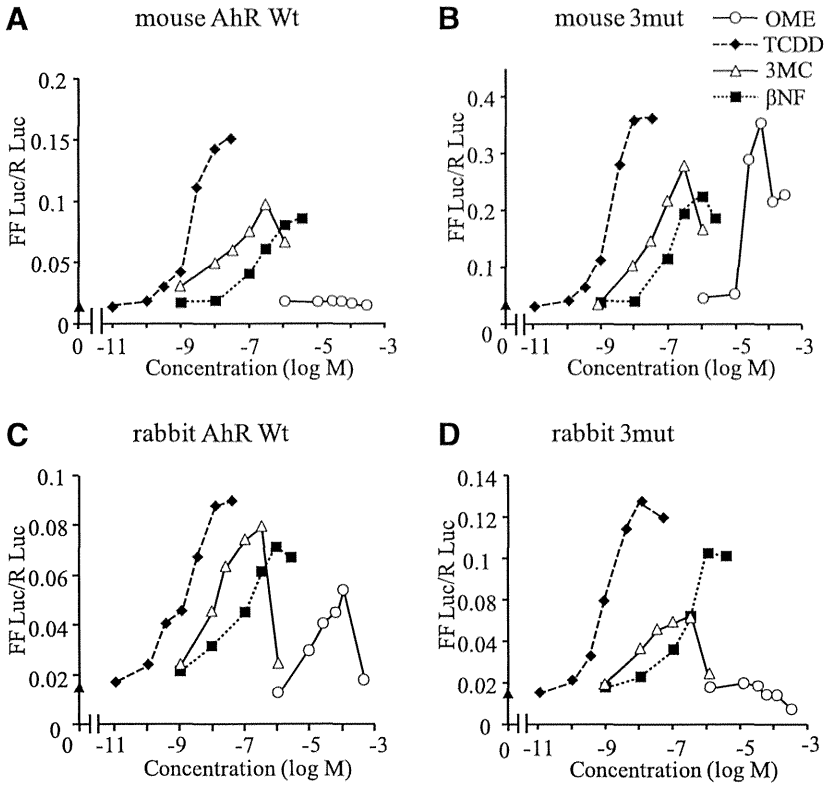

Fig. 10. Response of mouse and rabbit AhR mutants to OME, TCDD, 3MC, and β-naphthoflavone (β-NF). HeLa cells were transfected with reporter genes and (A) the mouse wild-type AhR (mouse AhR Wt); (B) the mouse AhR with the triple substitutions I324M, A349T, and L363F (mouse 3mut); (C) the rabbit wild-type AhR (rabbit AhR Wt); and (D) the rabbit AhR with the triple substitutions M328I, T353A, and F367L (rabbit 3mut). Open circles represent 1, 10, 25, 50, and 100 μM OME; solid diamonds represent 0.01, 0.1, 0.3, 1, 3, 10, and 20 nM TCDD; open triangles represent 1, 10, 30, 100, 200, and 1000 nM 3MC; and solid squares with dotted lines represent 1, 10, 100, 300, 1000, and 2000 nM β-NF. Data represent the means of normalized firefly luciferase (FFluc)/*Renilla* luciferase activities from two independent experiments. EC_{50} values were calculated and are summarized in Table 1.

effective alternative to the phenylalanine required for reconstituting the response to OME in the mouse AhR (Fig. 6). It is interesting that there are differences between Leu and Val despite their structural similarity. Ala at position 349 in the mouse AhR is also conserved in rat and hamster AhRs, which exhibit only a slight response to OME. In human and guinea pig AhRs, which are OME-sensitive, the corresponding amino acid at this position is threonine, identical to the rabbit AhR. Overall, these three amino acid residues correspond strongly to the species differences in the response to OME. The differences in intensity of the response to OME among the animal species can be explained well by this comparative approach.

The results of our study suggest some possibilities for elucidating the underlying mechanism of OME-mediated AhR activation. In our experiments, the response required an OME-sensitive AhR that depended on three amino acid residues located in LBD. Some reports have suggested that PTK is associated with OME-mediated AhR activation (Kikuchi et al., 1998; Backlund and Ingelman-Sundberg, 2005). In one report, the Y320 residue of the human AhR was determined to be a putative phosphorylation site required for OME responsiveness (Lemaire et al., 2004). However, this tyrosine residue and the proximal nine amino acids are conserved in all the AhRs tested in the present study. Furthermore, the three amino acid residues that we found to be essential are not putative phosphorylation sites, nor are they included in the PTK consensus. Hence, AhR phosphorylation by PTK may be influenced by a conformational change resulting from these three amino acids. The mutant AhRs generated in the present study will be useful for further investigations of the relationship between OME and PTK. Other than the involvement of PTK, a possible mechanism for OME-mediated AhR activation is the presence of some type of ligand. A possible type of ligand is an endogenous (intrinsic) ligand in the culture medium or one that is generated intracellularly. In general, an endogenous ligand is considered to be inactivated rapidly by P450 enzymes (Chang and Puga, 1998; Adachi et al., 2001; Spink et al., 2003). In the presence of a P450 inhibitor, the endogenous ligand remains and may activate the AhR. In fact, the inhibitory effects of OME on CYP1A1, 2C19, and 3A4 have been reported previously (Li et al., 2004; Shiizaki et al., 2008). By disrupting an autoregulatory loop consisting of CYP1A1 and FICZ, one of the endogenous ligands, a recent report showed that CYP1A1 upregulation by CYP1A1-inhibiting chemicals was due to an indirect mechanism (Wincent et al., 2012). On the basis of this finding, we confirmed CYP1A1 inhibition by OME (Fig. 1) and demonstrated that CYP1A1 activity was required for OME-mediated AhR activation (Fig. 2). These results were quite similar to the results obtained from CYP1A1 inhibitor

TABLE 1
Summary of EC_{50} values of endogenous and synthetic chemical ligands

	Mouse (wt)	Mouse (3mt)[a]	Rabbit (wt)	Rabbit (3mt)[b]
Omeprazole (μM)	NR	17.4	19.2	NR
TCDD (nM)	2.05	1.97	1.98	1.25
3MC (nM)	18.2	12.5	47.5	76.2
β-NF (nM)	167	188	218	272
FICZ (nM)	3.34	5.26	18.8	24.0
Kynurenic acid (μM)	8.74	9.73	13.1	12.8
ITE (nM)	30.5	38.4	19.9	36.7
Indirubin (nM)	358	187	131	138

β-NF, β-naphthoflavone; NR, no response observed; wt, wild-type.
[a]Mouse (3mt): mouse AhR containing I324M, A349T, and L363F substitutions.
[b]Rabbit (3mt): rabbit AhR containing M328I, T353A, and F367L substitutions.

Downloaded from molpharm.aspetjournals.org at ASPET Journals on November 18, 2014

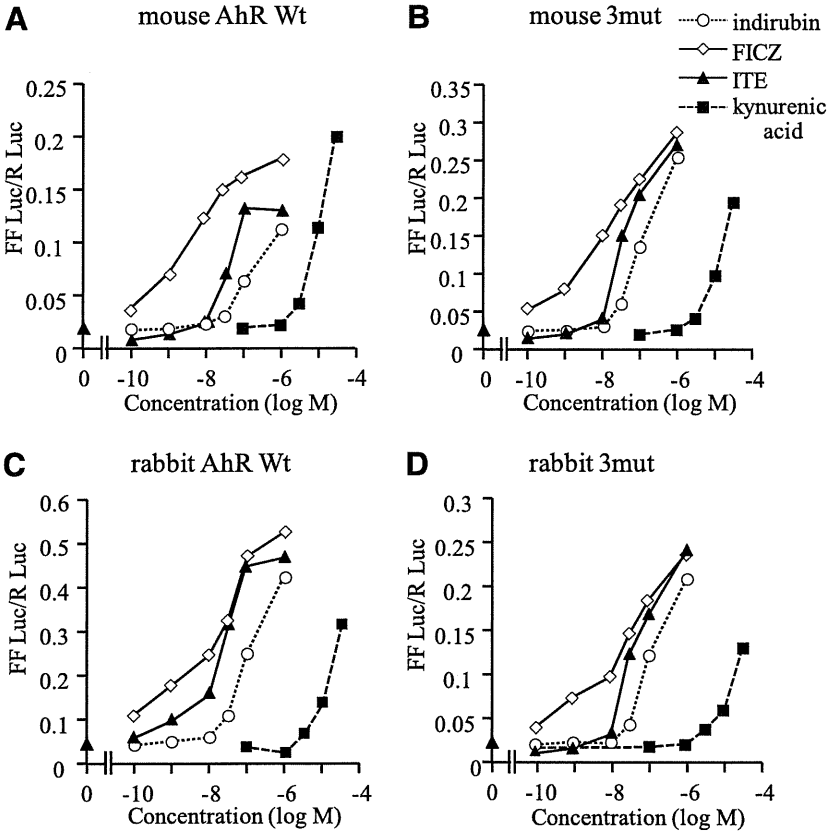

Fig. 11. Response of mouse and rabbit AhR mutants to known endogenous ligands: indirubin, FICZ, ITE, and kynurenic acid. HeLa cells were transfected with reporter genes and various AhRs: (A) the mouse wild-typeAhR (Mouse AhR Wt); (B) the mouse AhR with the triple substitutions I324M, A349T, and L363F (mouse 3mut); (C) the wild-type rabbit AhR (rabbit AhR Wt); and (D) rabbit AhR with the triple substitutions M328I, T353A, and F367L (rabbit 3mut). Open circles represent 0.1, 1, 10, 30, 100, and 1000 nM indirubin; open diamonds represent 0.1, 1, 10, 30, 100, and 1000 nM FICZ; solid triangles represent 0.1, 1, 10, 30, 100, and 1000 nM ITE; and solid squares represent 0.1, 1, 3, 10, and 30 μM kynurenic acid. Data represent the means of normalized firefly luciferase (FFluc)/*Renilla* luciferase activities from two independent experiments. EC_{50} values were calculated and are summarized in Table 1.

ellipticine. Furthermore, OME-mediated AhR activation was partially reduced as a result of charcoal-stripping of serum, which is considered to be a supplier of endogenous ligands (Fig. 3). Thus, we tested four putative endogenous ligands, including FICZ; however, AhR activation by these ligands was not significantly influenced by the three amino acid substitutions. We concluded that these four putative endogenous ligands are not involved in the indirect mechanism of OME-mediated AhR activation. Therefore, an enigmatic ligand may be involved. The possible mechanism related to the indirect activation of AhR by OME is illustrated in Supplemental Fig. 3. Another possible ligand is an unstable and short-lived metabolite of OME, which would be difficult to detect by general experimental procedures. Hu et al. developed a sensitive assay that indicated that OME itself could bind to AhR, although with a very low affinity (Hu et al., 2007). The results shown in Fig. 2 involve the possibility that CYP1A1 produces the putative active metabolite, and we do not have data that deny this hypothesis at present. If some ligand is related to OME-mediated AhR activation, it must differ in its affinity for rabbit and mouse AhRs, and the difference would be attributable to the three amino acid residues identified in this study.

In conclusion, three amino acids in the LBD of AhR define species-specific differences in OME-mediated AhR activation. These findings will be useful for elucidating the molecular mechanism underlying OME-mediated AhR activation.

Acknowledgments

The authors thank Dr. Kazuhiro Sogawa (Tohoku University, Japan) for providing the reporter plasmid pX4TK-Luc and Dr. Tomonari Matsuda (Kyoto University, Japan) for providing indirubin.

Authorship Contributions

Participated in research design: Shiizaki, Ohsako.

Conducted experiments: Shiizaki, Ohsako.

Contributed new reagents or analytic tools: Shiizaki, Ohsako, Kawanishi, Yagi.

Performed data analysis: Shiizaki.

Wrote or contributed to the writing of the manuscript: Shiizaki, Ohsako, Yagi.

References

Adachi J, Mori Y, Matsui S, Takigami H, Fujino J, Kitagawa H, Miller CA, 3rd, Kato T, Saeki K, and Matsuda T (2001) Indirubin and indigo are potent aryl hydrocarbon receptor ligands present in human urine. *J Biol Chem* **276**:31475–31478.

Backlund M and Ingelman-Sundberg M (2004) Different structural requirements of the ligand binding domain of the aryl hydrocarbon receptor for high- and low-affinity ligand binding and receptor activation. *Mol Pharmacol* **65**:416–425.

Backlund M and Ingelman-Sundberg M (2005) Regulation of aryl hydrocarbon receptor signal transduction by protein tyrosine kinases. *Cell Signal* **17**:39–48.

Backlund M, Johansson I, Mkrtchian S, and Ingelman-Sundberg M (1997) Signal transduction-mediated activation of the aryl hydrocarbon receptor in rat hepatoma H4IIE cells. *J Biol Chem* **272**:31755–31763.

Bohonowych JE and Denison MS (2007) Persistent binding of ligands to the aryl hydrocarbon receptor. *Toxicol Sci* **98**:99–109.

Burbach KM, Poland A, and Bradfield CA (1992) Cloning of the Ah-receptor cDNA reveals a distinctive ligand-activated transcription factor. *Proc Natl Acad Sci USA* **89**:8185–8189.

Chang CY and Puga A (1998) Constitutive activation of the aromatic hydrocarbon receptor. *Mol Cell Biol* **18**:525–535.

Curi-Pedrosa R, Daujat M, Pichard L, Ourlin JC, Clair P, Gervot L, Lesca P, Domergue J, Joyeux H, and Fourtanier G, et al. (1994) Omeprazole and lansoprazole are mixed inducers of CYP1A and CYP3A in human hepatocytes in primary culture. *J Pharmacol Exp Ther* **269**:384–392.

Daujat M, Peryt B, Lesca P, Fourtanier G, Domergue J, and Maurel P (1992) Omeprazole, an inducer of human CYP1A1 and 1A2, is not a ligand for the Ah receptor. *Biochem Biophys Res Commun* **188**:820–825.

Denison MS, Fisher JM, and Whitlock JP, Jr (1989) Protein-DNA interactions at recognition sites for the dioxin-Ah receptor complex. *J Biol Chem* **264**: 16478–16482.

Diaz D, Fabre I, Daujat M, Saint Aubert B, Bories P, Michel H, and Maurel P (1990) Omeprazole is an aryl hydrocarbon-like inducer of human hepatic cytochrome P450. *Gastroenterology* **99**:737–747.

DiNatale BC, Murray IA, Schroeder JC, Flaveny CA, Lahoti TS, Laurenzana EM, Omiecinski CJ, and Perdew GH (2010) Kynurenic acid is a potent endogenous aryl

Downloaded from molpharm.aspetjournals.org at ASPET Journals on November 18, 2014

hydrocarbon receptor ligand that synergistically induces interleukin-6 in the presence of inflammatory signaling. *Toxicol Sci* **115**:89–97.
Dzeletovic N, McGuire J, Daujat M, Tholander J, Ema M, Fujii-Kuriyama Y, Bergman J, Maurel P, and Poellinger L (1997) Regulation of dioxin receptor function by omeprazole. *J Biol Chem* **272**:12705–12713.
Ema M, Ohe N, Suzuki M, Mimura J, Sogawa K, Ikawa S, and Fujii-Kuriyama Y (1994) Dioxin binding activities of polymorphic forms of mouse and human arylhydrocarbon receptors. *J Biol Chem* **269**:27337–27343.
Fukunaga BN, Probst MR, Reisz-Porszasz S, and Hankinson O (1995) Identification of functional domains of the aryl hydrocarbon receptor. *J Biol Chem* **270**: 29270–29278.
Goryo K, Suzuki A, Del Carpio CA, Siizaki K, Kuriyama E, Mikami Y, Kinoshita K, Yasumoto K, Rannug A, and Miyamoto A, et al. (2007) Identification of amino acid residues in the Ah receptor involved in ligand binding. *Biochem Biophys Res Commun* **354**:396–402.
Hu W, Sorrentino C, Denison MS, Kolaja K, and Fielden MR (2007) Induction of cyp1a1 is a nonspecific biomarker of aryl hydrocarbon receptor activation: results of large scale screening of pharmaceuticals and toxicants in vivo and in vitro. *Mol Pharmacol* **71**:1475–1486.
Karchner SI, Franks DG, Kennedy SW, and Hahn ME (2006) The molecular basis for differential dioxin sensitivity in birds: role of the aryl hydrocarbon receptor. *Proc Natl Acad Sci USA* **103**:6252–6257.
Kennedy SW and Jones SP (1994) Simultaneous measurement of cytochrome P4501A catalytic activity and total protein concentration with a fluorescence plate reader. *Anal Biochem* **222**:217–223.
Kikuchi H, Fukushige S, Shibazaki M, and Shiratori Y (2002) Presence on human chromosome 10 of omeprazole-sensitivity gene whose product mediates CYP1A1 induction. *Cytogenet Genome Res* **97**:51–57.
Kikuchi H, Hossain A, Sagami I, Ikawa S, and Watanabe M (1995) Different inducibility of cytochrome P-4501A1 mRNA of human and mouse by omeprazole in culture cells. *Arch Biochem Biophys* **316**:649–652.
Kikuchi H, Hossain A, Yoshida H, and Kobayashi S (1998) Induction of cytochrome P-450 1A1 by omeprazole in human HepG2 cells is protein tyrosine kinase-dependent and is not inhibited by alpha-naphthoflavone. *Arch Biochem Biophys* **358**:351–358.
Kimura A, Naka T, Nohara K, Fujii-Kuriyama Y, and Kishimoto T (2008) Aryl hydrocarbon receptor regulates Stat1 activation and participates in the development of Th17 cells. *Proc Natl Acad Sci USA* **105**:9721–9726.
Krusekopf S, Kleeberg U, Hildebrandt AG, and Ruckpaul K (1997) Effects of benzimidazole derivatives on cytochrome P450 1A1 expression in a human hepatoma cell line. *Xenobiotica* **27**:1–9.
Lemaire G, Delescluse C, Pralavorio M, Ledirac N, Lesca P, and Rahmani R (2004) The role of protein tyrosine kinases in CYP1A1 induction by omeprazole and thiabendazole in rat hepatocytes. *Life Sci* **74**:2265–2278.
Li XQ, Andersson TB, Ahlström M, and Weidolf L (2004) Comparison of inhibitory effects of the proton pump-inhibiting drugs omeprazole, esomeprazole, lansoprazole, pantoprazole, and rabeprazole on human cytochrome P450 activities. *Drug Metab Dispos* **32**:821–827.
Lind T, Cederberg C, Ekenved G, Haglund U, and Olbe L (1983) Effect of omeprazole—a gastric proton pump inhibitor—on pentagastrin stimulated acid secretion in man. *Gut* **24**:270–276.
Mimura J, Ema M, Sogawa K, and Fujii-Kuriyama Y (1999) Identification of a novel mechanism of regulation of Ah (dioxin) receptor function. *Genes Dev* **13**:20–25.
Murray IA, Morales JL, Flaveny CA, Dinatale BC, Chiaro C, Gowdahalli K, Amin S, and Perdew GH (2010) Evidence for ligand-mediated selective modulation of aryl hydrocarbon receptor activity. *Mol Pharmacol* **77**:247–254.
Murray IA, Reen RK, Leathery N, Ramadoss P, Bonati L, Gonzalez FJ, Peters JM, and Perdew GH (2005) Evidence that ligand binding is a key determinant of Ah receptor-mediated transcriptional activity. *Arch Biochem Biophys* **442**:59–71.
Pollenz RS, Sattler CA, and Poland A (1994) The aryl hydrocarbon receptor and aryl hydrocarbon receptor nuclear translocator protein show distinct subcellular localizations in Hepa 1c1c7 cells by immunofluorescence microscopy. *Mol Pharmacol* **45**:428–438.
Quattrochi LC and Tukey RH (1993) Nuclear uptake of the Ah (dioxin) receptor in response to omeprazole: transcriptional activation of the human CYP1A1 gene. *Mol Pharmacol* **43**:504–508.
Quintana FJ, Basso AS, Iglesias AH, Korn T, Farez MF, Bettelli E, Caccamo M, Oukka M, and Weiner HL (2008) Control of $T_{(reg)}$ and $T_{(ID)}17$ cell differentiation by the aryl hydrocarbon receptor. *Nature* **453**:65–71.
Reyes H, Reisz-Porszasz S, and Hankinson O (1992) Identification of the Ah receptor nuclear translocator protein (Arnt) as a component of the DNA binding form of the Ah receptor. *Science* **256**:1193–1195.
Shiizaki K, Ohsako S, Kawanishi M, and Yagi T (2008) Omeprazole alleviates benzo [a]pyrene cytotoxicity by inhibition of CYP1A1 activity in human and mouse hepatoma cells. *Basic Clin Pharmacol Toxicol* **103**:468–475.
Shiizaki K, Ohsako S, Koyama T, Nagata R, Yonemoto J, and Tohyama C (2005) Lack of CYP1A1 expression is involved in unresponsiveness of the human hepatoma cell line SK-HEP-1 to dioxin. *Toxicol Lett* **160**:22–33.
Song J, Clagett-Dame M, Peterson RE, Hahn ME, Westler WM, Sicinski RR, and DeLuca HF (2002) A ligand for the aryl hydrocarbon receptor isolated from lung. *Proc Natl Acad Sci USA* **99**:14694–14699.
Spink BC, Hussain MM, Katz BH, Eisele L, and Spink DC (2003) Transient induction of cytochromes P450 1A1 and 1B1 in MCF-7 human breast cancer cells by indirubin. *Biochem Pharmacol* **66**:2313–2321.
Wei YD, Helleberg H, Rannug U, and Rannug A (1998) Rapid and transient induction of CYP1A1 gene expression in human cells by the tryptophan photoproduct 6-formylindolo[3,2-b]carbazole. *Chem Biol Interact* **110**:39–55.
Wincent E, Bengtsson J, Mohammadi Bardbori A, Alsberg T, Luecke S, Rannug U, and Rannug A (2012) Inhibition of cytochrome P4501-dependent clearance of the endogenous agonist FICZ as a mechanism for activation of the aryl hydrocarbon receptor. *Proc Natl Acad Sci USA* **109**:4479–4484.
Yoshinari K, Ueda R, Kusano K, Yoshimura T, Nagata K, and Yamazoe Y (2008) Omeprazole transactivates human CYP1A1 and CYP1A2 expression through the common regulatory region containing multiple xenobiotic-responsive elements. *Biochem Pharmacol* **76**:139–145.

Address correspondence to: Takashi Yagi, Department of Biology, Graduate School of Science, Osaka Prefecture University, 1-2 Gakuen-cho, Naka-ku, Sakai, Osaka, Japan. E-mail: yagi-t@riast.osakafu-u.ac.jp

Downloaded from molpharm.aspetjournals.org at ASPET Journals on November 18, 2014

Acta Histochemica 116 (2014) 474–480

Contents lists available at ScienceDirect

Acta Histochemica

journal homepage: www.elsevier.de/acthis

Single administration of butylparaben induces spermatogenic cell apoptosis in prepubertal rats

Mohammad Shah Alam[a,b], Seiichiroh Ohsako[c], Yoshiakira Kanai[b], Masamichi Kurohmaru[b,*]

[a] Department of Anatomy and Histology, Faculty of Veterinary Medicine and Animal, Science, Bangabandhu Sheikh Mujibur Rahman Agricultural University, Gazipur 1706, Bangladesh
[b] Department of Veterinary Anatomy, Graduate School of Agricultural and Life Sciences, The University of Tokyo, 1-1-1 Yayoi, Bunkyo-ku, Tokyo 113-8657, Japan
[c] Laboratory of Environmental Health Sciences, Center for Disease Biology and Integrative Medicine, Graduate School and Faculty of Medicine, The University of Tokyo, 7-3-1 Hongo, Bunkyo-Ku, Tokyo 113-0033, Japan

ARTICLE INFO

Article history:
Received 30 August 2013
Received in revised form 5 October 2013
Accepted 6 October 2013

Keywords:
Butylparaben
Prepubertal stage
Spermatogenic cell apoptosis
Rat

ABSTRACT

Parabens are *p*-hydroxybenzoic acid ester compounds widely used as preservatives in foods, cosmetics, toiletries and pharmaceuticals. Some parabens, including butylparaben, exert an estrogenic activity as determined by *in vitro* estrogen receptor assay and *in vivo* uterotrophic assay, and adversely affect endocrine secretion and male reproductive function. We conducted a research study to evaluate the acute effects of butylparaben on testicular tissues of prepubertal rats. Three-week-old male rats ($n=8$) were given a single dose of 1000 mg/kg butylparaben. The rats were sacrificed under anesthesia at 3, 6 and 24 h after administration, and their testes were collected for histopathological examination. The study revealed progressive detachment and sloughing of spermatogenic cells into the lumen of the seminiferous tubules at 3 h, and this effect was enhanced at 6 h after administration. Thin seminiferous epithelia and wide tubular lumina were seen at 24 h in the butylparaben-treated group, compared to the control. In order to clarify whether sloughed spermatogenic cells underwent apoptosis, TUNEL assay was carried out. We found a significant increase in the number of apoptotic spermatogenic cells in all the treated groups, compared to the controls and a maximal number of apoptotic cells were detected at 6 h after administration. In semithin sections, apoptotic cells were easily detected by their prominent basophilia and condensed chromatin, mainly found in spermatocytes. Ultrastructurally, the condensed chromatin and shrunken cytoplasm and nucleus, hallmarks of apoptotic cell death, were observed in butylparaben-treated groups. These observations lead us to postulate that butylparaben, similar to other estrogenic compounds, also induces spermatogenic cell apoptosis.

© 2013 Published by Elsevier GmbH.

Introduction

Parabens are a group of alkyl esters of *p*-hydroxybenzoic acid and typically include methylparaben, ethylparaben, propylparaben, butylparaben, isobutylparaben, isopropylparaben, and benzylparaben. Humans are exposed to these parabens *via* personal care products, owing to their extensive use in cosmetics, toiletries, food, and pharmaceuticals. Upon dietary exposure, parabens are rapidly hydrolyzed in the gut by esterases to different metabolites (Derache and Gourdon, 1963). In several *in vitro* studies, parabens were able to bind to estrogen receptors (ERs), activating genes controlled by hormones *via* the receptor (Byford et al., 2002; Pugazhendhi et al., 2005; Prusakiewicz et al., 2007). Administration of butylparaben has also been shown to increase uterine weight *in vivo* in both immature rats and mice and in adult ovariectomized mice, hence confirming its estrogenic activity (Soni et al., 2005; Routledge et al., 1998).

Prepubertal mice (4-weeks-old) treated with butylparaben for 10 weeks showed a dose-dependent decrease of both round and elongated spermatid counts and serum testosterone levels in all the treated groups (Oishi, 2002). It was further demonstrated (Oishi, 2004) that decreased testicular testosterone levels caused alterations of male reproductive function in prepubertal rats after propylparaben administration for 7 days. Nevertheless, it was also shown that neither male reproductive functions nor serum hormone levels including testosterone, LH and FSH were affected by methylparaben and ethylparaben at a dose of about 1000 mg/kg/day (Oishi, 2004).

* Corresponding author.
E-mail address: amkuroh@mail.ecc.u-tokyo.ac.jp (M. Kurohmaru).

0065-1281/$ – see front matter © 2013 Published by Elsevier GmbH.
http://dx.doi.org/10.1016/j.acthis.2013.10.006

It has been reported that *in utero* exposure of butylparaben decreased steroidogenesis by interfering with the transport of cholesterol to mitochondria (Taxvig et al., 2008). In another study (Song et al., 1991) showed that butylparaben exerts an inhibitory effect on the acrosomal enzyme acrosin, and impairs sperm membrane function, suggesting that spermatogenic cells could be a target of parabens in the testis (Tavares et al., 2009). As far as we are aware there are no published reports regarding spermatogenic cell apoptotic index induced by parabens.

It has been demonstrated that several environmental endocrine disruptors have activities similar to those of endogenous estrogen (17β-estradiol) or antiandrogens, including bisphenol A (vom Saal et al., 1998), alkylphenol (Routledge and Sumpter, 1997) and phthalates (Alam et al., 2010b). These estrogenic compounds can cause alterations in circulating concentrations of gonadotropins (LH, FSH) and testicular testosterone, and thus can interfere with spermatogenesis. In previous studies in prepubertal rats we demonstrated that a single dose of estrogenic compounds, such as di(*n*-butyl) phthalate and estradial-3-benzoate, inhibits testicular steroidogenesis and decreases serum LH and FSH levels, together with significantly increasing spermatogenic cell apoptosis (Alam et al., 2010b). Many of the parabens, including butylparaben, are thought to possess estrogenic activity leading to reduced testosterone levels and lower counts of both round and elongated spermatids (Routledge et al., 1998; Pedersen et al., 2000; Okubo et al., 2001; Byford et al., 2002; Oishi, 2002; Taxvig et al., 2008). In the present study, we investigated histochemically the possible acute effects of butylparaben on testes at prepubertal stage on apoptotic inducibility, which is a specific feature of estrogenic compounds.

Materials and methods

Chemicals

Butylparaben (purity > 99% purity) was purchased from Wako Pure Chemical Industries (Osaka, Japan). Proteinase K and 3,3′-diaminobenzidine tetrahydrochloride (DAB) were from TaKaRa (Otsu, Japan). Neutral buffered formalin and propylene oxide were from Wako. Osmium tetroxide and Araldite M were from Nisshin EM Co. (Tokyo, Japan). The terminal deoxy-nucleotidyl transferase-mediated digoxigenin-dUTP nick-end labeling (TUNEL) (*In Situ* Apoptotic Detection) Kit was purchased from TaKaRa.

Animals and treatments

Male Sprague-Dawley rats (3-weeks-old) were purchased from Charles River Laboratories (Tokyo, Japan). The rats were housed three to five per plastic cage, maintained on a 12 h light/dark cycle at a constant temperature (22 °C ± 1 °C) and humidity (45–70%), and provided water and rodent pellets (Oriental Yeast, Tokyo, Japan) *ad libitum*. Animals were maintained and handled humanely in accordance with the guidelines on animal experiments of the Institutional Animal Care and Use Committee (IACUC) of the University of Tokyo, Tokyo, Japan. Three-week-old male rats ($n = 8$) were given a single oral administration of 1000 mg/kg butyloaraben in vehicle at a volume equal to 4 ml/kg. The vehicle was a mixture of 5% ethanol and 95% corn oil. Control animals received the same volume of vehicle. Rats were then killed under diethyl ether anesthesia at 3, 6 and 24 h after administration, and their testes were collected and subjected to histopathology.

Light microscopy

For histopathological observations (hematoxylin and eosin, TUNEL), under diethyl ether anesthesia, rats were perfused with 10% neutral buffered formalin for 30 min. Following perfusion, the testes were excised and immersed in the same fixative for 48 h. Then, the samples were washed in 0.1 M phosphate buffer solution for 3 h, dehydrated through a graded series of ethanol, cleared in xylene, and embedded in paraffin. Sections from the paraffin blocks were cut at 4 μm in thickness. The sections were then stained with Meyer's hematoxylin and eosin (H&E) and/or periodic acid-Schiff (PAS)-hematoxylin (Wako, Osaka, Japan). The samples were studied with an Olympus (BX50) light microscope (Tokyo, Japan).

TUNEL assay

In order to quantitatively assess the incidence of apoptotic spermatogenic cells after treatment, *in situ* terminal deoxynucleotidyl transferase-mediated digoxigenin-dUTP nick-end-labeling (TUNEL) assay was performed using an Apoptotic Detection Kit according to the manufacturer's instructions. Briefly, the testes sections were deparaffinized and digested with 10 μg/ml proteinase K at 37 °C for 15 min. After being washed three to five times with 0.01 M phosphate buffer solution (PBS, pH7.4), they were treated with terminal deoxynucleotidyl transferase (TdT) enzyme and Labeling Safe Buffer, which were included in the kit. The TdT reaction was conducted at 37 °C for 90 min. To check for the non-specific reaction, the sections were incubated with PBS alone instead of FITC-labeled TdT enzyme. After further washing three to five times with PBS, they were incubated with horseradish peroxidase (HRP) goat anti-biotin at 37 °C for 30 min. The localization of HRP sites was determined by application of DAB. The sections were then counterstained with methyl green and mounted. Images of seminiferous tubules were obtained by using an Olympus (BX50) light microscope connected to a digital camera (DP20, Olympus, Tokyo, Japan). Using a ×20 objective, 3 fields in each section were randomly selected. The area of seminiferous tubules in all fields was measured by a computer assisted system using Scion Image software (Scion Co., Frederick, MD, USA). Then, TUNEL-positive (brown-stained) spermatogenic cells in all selected areas were counted. The number of TUNEL-positive cells per 1 mm^2 seminiferous tubule was calculated as described in our previous study (Alam et al., 2010b). Data were obtained from 4 rats in each group and were given as mean ± S.E.M.

Transmission electron microscopy

For transmission electron microscopy, under diethyl ether anesthesia, rats were perfused with 5% glutaraldehyde in 0.1 M phosphate buffer, and then the testes were excised, immersed in the same fixative at 4 °C for 3 h and postfixed in 1% osmium tetroxide (OsO_4) at 4 °C for 2 h. The samples were then dehydrated in ethanol, infiltrated in propylene oxide, and embedded in Araldite M. Semi-thin sections were cut at 1 μm in thickness, stained with 1% toluidine blue, and observed by light microscopy. Ultrathin sections were cut, and stained with uranyl acetate and lead citrate. In the butylparaben-treated rats, unique lesions were encountered at the light microscopic level at 24 h. Corresponding tissue sections from these animals, along with appropriate control sections, were examined using a JEM-1010 transmission electron microscope at 80 kV (JEOL, Tokyo, Japan). Evaluation was limited to characterization of subtle lesions and abnormal cells, because quantitative analysis is very limited with electron microscopy.

Statistical analysis

Statistical analysis was performed using Stat View software (SAS Institute Inc., Cary, NC, USA). All results are represented as the means ± S.E.M. For the comparison of apoptotic spermatogenic cell index, one-way analysis of variance (ANOVA) was carried out followed by Fisher's PLSD as a *post hoc* test. Differences were

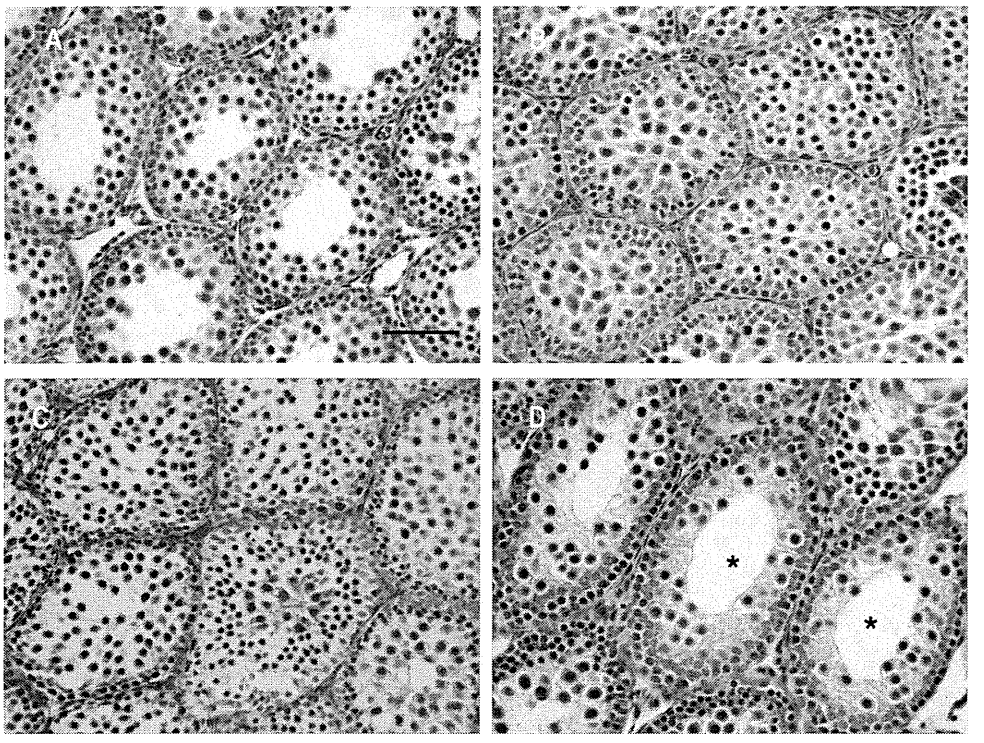

Fig. 1. Histopathological changes in testes after single administration of 1000 mg/kg butylparaben are shown. Control of vehicle administration at 24 h (A). Reduction of tubular lumen due to detachment and displacement of spermatogenic cells at 3 h after administration (B), Sloughing of spermatogenic cells at 6 h (C). Thin seminiferous epithelia and wide tubular lumen (*) at 24 h (D). Scale bar = 50 μm.

considered to be statistically significant when the *P* value was less than 0.05.

Results

Histopathology

Histopathology was evaluated using cross-sections of seminiferous tubules stained with hematoxylin and eosin by light microscopy. Due to progressive detachment and sloughing of spermatogenic cells into the lumen of the seminiferous tubules, reduction and/or disappearance of tubular lumen was observed at 3 h after butylparaben treatment (Fig. 1B). This effect was enhanced at 6 h since Sertoli cells and spermatogonia with few spermatocytes remained within the seminiferous tubules (Fig. 1C). Thin seminiferous epithelia and wide tubular lumen were recognized at 24 h (Fig. 1D) after butylparaben treatment, compared to the vehicle treated control at 24 h (Fig. 1A). Since in all time schedules, the vehicle-treated control had the same manner of seminiferous epithelia structure, the longest period (24 h) of vehicle treated group was chosen for the control (Fig. 1A).

Apoptosis

We carried out a TUNEL assay to detect whether sloughed spermatogenic cells were undergoing apoptosis. We found a significant increase in the number of apoptotic spermatogenic cells in the treated groups in comparison with the control group (Fig. 2). The maximal number of apoptotic spermatogenic cells was detected at 6 h after treatment (Fig. 2C and E). At 24 h after administration, the number of apoptotic cells began to gradually decline, though it was still significantly greater than that in the control group (Fig. 2D and E). In order to evaluate the spermatogenic cell types that underwent apoptosis, apoptotic cells were analyzed by light microscopy (semithin sections) and transmission electron microscopy. In semithin sections stained with toluidine blue, degenerative spermatogenic cells were easily detected by their prominent basophilia, condensed nuclear chromatin and shrinkage of cytoplasm (Fig. 3A–D). Apoptotic spermatogenic cells were frequently observed in the butylparaben-treated group, compared with the control group (Fig. 3). Close observations showed the apoptotic (nuclear chromatin condensed) cells were rounded-up and surrounded by an empty space. They might separate from their neighbors. Spermatocytes were the largest cells and showed typically dispersed chromatin, and spermatogonia were identified by their location (within the basal compartment, among the Sertoli cells). Similarly, at the transmission electron microscopic level, the condensed chromatin and shrinkage of cytoplasm and nucleus were observed. The apoptotic spermatocytes might be phagocytosed by neighboring Sertoli cells (Fig. 3F). These data indicate that butylparaben induces apoptotic cell death in testes and is most commonly found in spermatocytes, less frequently in spermatids, and not in spermatogonia and somatic cells (Sertoli cells or Leydig cells).

Discussion

We used prepubertal rats in the present study and observed the testicular alterations after a single administration of butylparaben. The prepubertal stage is much more sensitive than adults (Kondo et al., 2006), and rats are more sensitive to endocrine disruptors than mice. A massive number of spermatogenic cells undergo apoptosis in the first wave of spermatogenesis (first to seven weeks of postnatal life), and the highest rate of apoptosis occurs at 18–26 days of age to maintain an optimum Sertoli and spermatogenic cells ratio (Yan et al., 2000). Apoptosis is a process of cell death and is involved in various physiological and pathological events (Saikumar et al., 1999). During various stages of mammalian spermatogenesis, spermatogenic cell apoptosis occurs to remove abnormal spermatogenic cells and to maintain normal quantity and quality of sperm afterwards (Billig et al., 1995; Print and Loveland,